Genotypic and phenotypic analysis of plant-associated *Pseudomonas*

A thesis submitted in partial fulfilment of the requirements for the degree of

Master of Science

in

Environmental Microbiology

at Massey University, Auckland, New Zealand.

Hao Chang

2011

Abstract

The ecological success of *Pseudomonas* in plant environments is largely determined by the phenotypes that it expresses: efficient utilization of plant-derived nutritional substrates is fundamentally important for bacterial competitive growth. Not surprisingly then, *Pseudomonas* up-regulates the expression of many genes involved in nutrient scavenging when colonizing the plant surfaces. A typical example is the *hut* genes dedicated to the utilization of histidine and urocanate (the first intermediate of the histidine degradation pathway) in the model organism of *P. fluorescens* SBW25. Previous work has defined the genes involved in the histidine/urocanate uptake, degradation and regulation. This study aims to extend our understanding of histidine/urocanate utilization to the population level.

A total of 230 *Pseudomonas* strains were isolated from the phyllosphere of sugar beets grown in Oxford (UK) and Auckland (New Zealand) and their ability to grow on histidine and urocanate was tested. The results revealed considerable variation of phenotypes, for example, strains were capable of growing on histidine but not on urocanate (His^+, Uro^-, 11%) and vice versa (His^-, Uro^+, 13%). Interestingly, His^+, Uro^- strains were commonly found in the Auckland population, whereas His^-, Uro^+ strains were more prevalent in the Oxford population. Introduction of cloned copies of the histidine- and urocanate-specific transporter genes (*hutTh* and *hutTu)* from *P. fluorescens* SBW25 restored the ability of many naturally His^- and Uro^- strains to utilize histidine and urocanate, respectively. Together, the data indicate that *Pseudomonas* populations are polymorphic with respect to the transporters.

The genetic relatedness of the two *Pseudomonas* populations from Oxford and Auckland was estimated using multi-locus sequence analysis (MLSA) of three genes (*gapA*, *gltA* and *acnB*). For each of the three genes, oligonucleotide primers were designed to amply the DNA fragment (~600 nt) which was subjected to subsequent DNA sequencing. The DNA sequences of three genes (615 nt for *gltA*, 303 nt for *gapA*, 273 nt for *acnB*) were concatenated and used for phylogenetic analysis. Results showed that the *Pseudomonas* population

from Auckland is phylogenetically distinct from that of Oxford; there is a clear correlation between the MLSA genotypes and the phenotypes (i.e., utilization of histidine vs. urocanate).

Taken together, my data show that the two *Pseudomonas* populations colonizing the phyllosphere of sugar beets in Oxford and Auckland are genetically diverse and display distinct phenotypes in terms of their ability to grow on histidine and urocanate as the sole source of carbon and nitrogen. Furthermore, the observed phenotypic diversity is attributable to variation in histidine- and urocanate-specific transports, not genes for histidine catabolism.

[Of note, the results reported in this thesis on the polymorphism of histidine and urocanate utilization in plant-associated *Pseudomonas* has been published in the journal of *Environmental Microbiology*, wherein I am the second author (see Appendix B).]

Acknowledgements

First of all, I would like to take this opportunity to thank my principle supervisor, Dr. Xue-Xian Zhang, for his kindness support and endless helps and guidance. Without him, I would not have had this opportunity.

I would like to thank Prof. Paul Rainey of being my co-supervisor. Thank you for your knowledge, expertise, limitless encouragements and helps throughout these years. I really enjoyed being a member in the Rainey Lab.

Thanks must go to Dr. Austen Ganley and Dr. Wayne Patrick, for being my friendly colleagues for any discussions, and thank you for lecturing me.

I would like to acknowledge Dr. Eric Libby and Dr. Steve Ritchie for helping me with data analysis and discussions, without which, none of this would be possible.

Many big thanks to everyone in the Rainey Lab for making here such a good place to work and study. Thanks to Jonathan, Yunhao, Jenna, Christian, Frederic, for being there at the times when I had questions, and being friends in my life.

I am most grateful for the unconditional love and financial support received from my parents over the years. Without you I would not have gone this far.

Table of Contents

Table of Abbreviations

Abbreviation	Meaning
µl	microlitre
BLAST	basic local alignment search tool
bp	base pairs
dNTP	dinucleotide triphosphate
h	hour
IPTG	isopropyl-β-D-thiogalactoside
kb	kilobase pairs
Km	kanamycin
LB	luria-bertaini
g	gram/gravity
His	histidine
Uro	urocanate
M	molar
mg	milligram
nt	nucleotide
min	minute
OD	optical density
nm	nanometre
PCR	polymerase chain reaction
rpm	rotation per minute
NF	nitrofurantonin
TBE	tris-borate-EDTA
Tc	tetracycline
Gen	gentamicin
UV	ultraviolet
X-gal	5-bromo-4-chloro-3-indolyl-beta-D-galactopyranoside
MLSA	multi-locus sequence analysis
LCMSMS	liquid chromatography-mass spectrometry
HPLC	high pressure liquid chromatography
WT	wild type
ICP-MS	Inductively Coupled Plasma Mass Spectrometry

Chapter 1: Introduction

1.1 Diversity of bacterial strains in the genus of *Pseudomonas*

The genus *Pseudomonas* encompasses a large group of phenotypically and genetically diverse saprophytic bacteria (Haubold and Rainey 1996; Mulet et al. 2010). Members of the genus are metabolically versatile and present in large numbers in terrestrial, freshwater and marine environments. Significantly, several species form intimate associations with eukaryotic hosts (plants and animals). As efficient plant colonizers, strains of some species (e.g., *P. syringae*) can cause plant disease, whereas others such as strains of *P. fluorescens* and *P. putida* can enhance the plant health. The ubiquitous distribution of *Pseudomonas* suggests their remarkable adaptability to different environmental conditions. Consequently, the genus currently contains 118 species and the number is still growing (Stanier et al. 1966; Palleroni 2010).

Evidence of phenotypic diversity in *Pseudomonas* can be dated back to early biochemical analysis led by Stanier, Palleroni and Doudoroff (Palleroni 2010). In a milestone paper published in 1966, they reported phenotypic characterization of 267 strains whereby their ability to utilize 146 different organic compounds as the sole source of carbon and energy was assessed (Stanier et al. 1966b). Because of the availability of massive phenotypic data, *Pseudomonas* species are traditionally identified by physiological profiling. For example, *Pseudomonas* strains give positive result in the oxidase test; most strains also produce the fluorescent yellow-green siderophore, pyoverdine, on iron-depleted medium (thus generally called fluorescent pseudomonads).

Later molecular analyses, mainly 16S rDNA phylogeny, have greatly shaped the *Pseudomonas* taxonomy and as a result, some former *Pseudomonas* species were relocated into other genera. Although the core groups described by Stanier et al. (1966) remain unchanged, bacteria in the *Pseudomonas* genus still display a high degree of diversity.

Sequence analysis of 16S rRNA genes is a powerful tool for genus assignment but it cannot provide sufficient information on discrimination of bacterial strains at the species level. Recent studies of *Pseudomonas* phylogeny have thus focused on the utilization of alternative molecular marker genes such as *recA*, *atpD, carA, gyrB, rpoB and rpoD* (Zhang and Rainey 2007; Waine et al. 2009). More recently, Mulet et al. examined the phylogenetic relationships among type strains of 107 *Pseudomonas* species by partial sequence analysis of four house-keeping genes (*gyrB, rpoB* and *rpoD* plus the 16S rDNA) (Mulet et al. 2010). The data suggests that the *Pseudomonas* genus can be divided into two lineages or intrageneric groups: one is represented by the human pathogenic bacteria *P. aeruginosa* and the other represented by "fluorescent pseudomonads" with *P. fluorescens* as the dominant group.

Of particular note is the techniques used in those phylogenetic studies (Zhang and Rainey 2007; Waine et al. 2009; Palleroni 2010), which are known as multilocus sequence analysis (MLSA) or multilocus sequence typing (MLST) (Maiden et al. 1998). The MLSA analysis involves sequence comparison of a set of "house-keeping" genes (usually 3-7 genes, depending on the levels of discrimination desired). These genes are highly conserved compared to normal protein-encoding genes but evolve more rapidly than the rRNA genes. An internal region (~ 400 nt) of each house-keeping gene can be accurately sequenced by a standard procedure of PCR-amplification followed by DNA sequencing. For each house-keeping gene, different sequences represent distinct alleles; sequence variations at different loci define the allelic profile of each bacterial isolate. Therefore, MLSA is the most advanced analytic tool to measure the genetic relatedness of closely related bacterial strains.

The genetic structure of a bacterial population is linked to the evolutionary processes of mutation, recombination, migration, natural selection and genetic drift. The MLSA data of DNA sequence variation at different loci make it possible to assess how the bacterial population is shaped by these evolutionary processes. Given the ecological and economic significance of *Pseudomonas* strains, there have been numerous reports on phenotypic and phylogenetic

diversity of *Pseudomonas* strains (Rainey et al. 1994; Haubold and Rainey 1996; Rainey 1999; Joardar et al. 2005; Khan et al. 2008). However, only a handful of studies have analyzed the population structure of *Pseudomonas* strains using MLSA of these, the majority have focused on evolutionary relationships among the human pathogenic *P. aeruginosa*. No MLSA analysis has been done on a locally adapted *Pseudomonas* population, e.g. strains isolated from plants grown in the same field.

1.2 Utilization of histidine and its derivate (urocanate) by plant-associated *Pseudomonas*

Many plant-associated *Pseudomonas* strains (e.g., *P. fluorescens* SBW25) are capable of growing on histidine as the sole source of carbon and/or nitrogen (Zhang and Rainey 2007). As shown in Fig. 1.1, histidine degradation in *Pseudomonas* is mediated by a five-step pathway with glutamate, formate and ammonia being the end products (Revel and B Magasanik 1958; Hug et al. 1968; Coote and Hassall 1973; Allison and Phillips 1990; Cook 2001). The first step from histidine to urocanate is catalyzed by histidine ammonia lyase (histidase), the gene product of *hutH*. Urocanate is then converted to imidazolone propionate (IPA) by the enzyme urocanase encoded *hutU*. IPA is then hydrolyzed to form formiminoglutamate (FIGLU) by imidazolone propionate hydrolase (IPAase) encoded by *hutI*. Further degradation of FIGLU differs in *Pseudomonas* and enteric bacteria. In enteric bacteria such as *Salmonella typhimurium* and *Klebsiella aerogenes*, FIGLU is directly hydrolyzed to form glutamate, formamide and one ammonium via a four-step pathway. However, in *Pseudomonas* FIGLU is converted to glutamate, formate, and ammonia by two enzymes - iminohydrolase encoded by *hutF* and formylglutamase encoded by *hutG* – with formyl-glutamate (FG) as the intermediate compound. Notably, formate can serve the cell as a donor of single carbon, whereas formamide cannot be further metabolized and leaks outside the cell (Fernandez et al. 2004; Itoh et al. 2007).

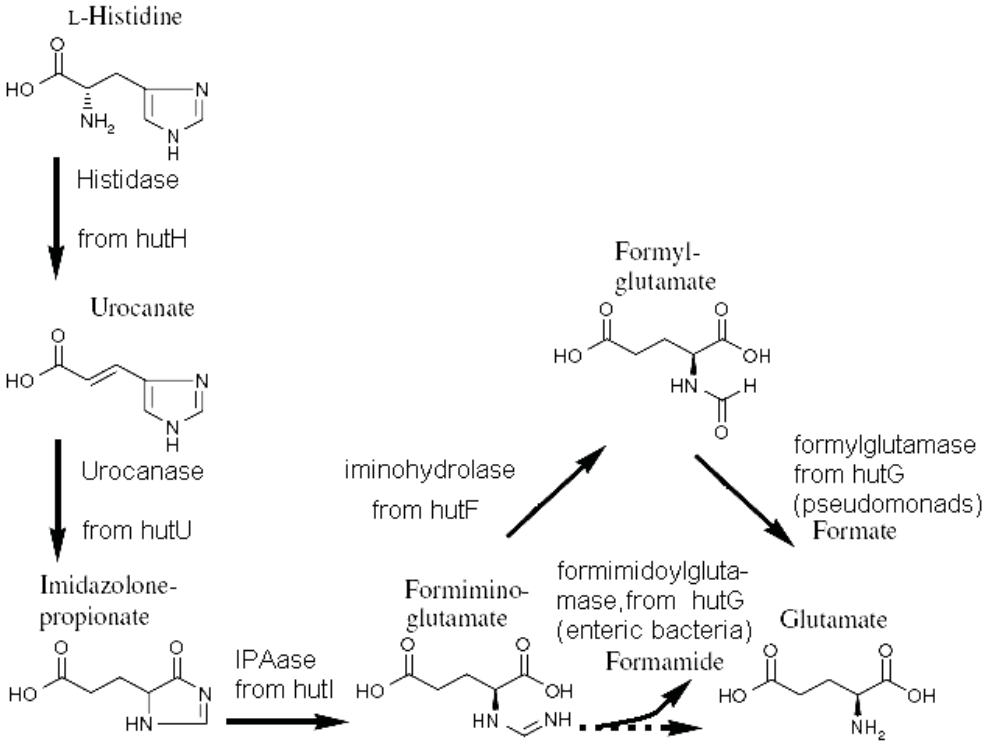

Fig. 1.1. Histidine catabolic pathways. The *hut* gene products are listed beside arrows. The first 3 steps: histidine to urocanate, urocanate to imidazolone propionate (IPA), and IPA to formimino-glutamate (FIGLU) are conserved between *Pseudomonas* species. Enteric bacteria hydrolyse FIGLU directly to form glutamate, one ammonia and formamide (indicated by the dot arrow), pseudomonads have the additional step to form formylglutamate (FG), two ammonia and formate.

As shown in *P. fluorescens SBW25*, *hut* genes are arranged in 3 transcriptional units or operons: *hutF, hutCD* and ten genes from *hutU* to *hutG* (Fig. 1.2). Transcription of the *hut* operon is regulated by the repressor protein *hutC*. Interestingly, many bacteria, including *P. fluorescens* SBW25, can grow on urocanate – the first intermediate of the *hut* pathway – as the sole source of carbon and/or nitrogen (Hu and Phillips 1988; Hu et al. 1989; Zhang and Rainey 2007). Urocanate is the direct inducer of the *hut* operon: urocanate (not histidine) is capable of binding to the *hutC* repressor protein causing *hutC* to dissociate from the operator site (Allison and Phillips 1990). Histidine-induced *hut* expression thus requires functional *hutH* to produce the inducer from histidine.

Except genes involved in the breakdown of histidine and urocanate, utilization also requires functional transport systems for the uptake of the nutrients from the external environments. Recent work by Zhang, et al. (Zhang et al. 2011) led

to the identification of genes encoding the histidine- and urocanate-specific transporter. As indicated in Fig. 1.2., *hutTh* encodes the major high-affinity histidine transporter; *hutTu* encodes an urocanate-specific transporter; *hutXWV* encodes an ABC-type transporter that plays a minor role in histidine uptake.

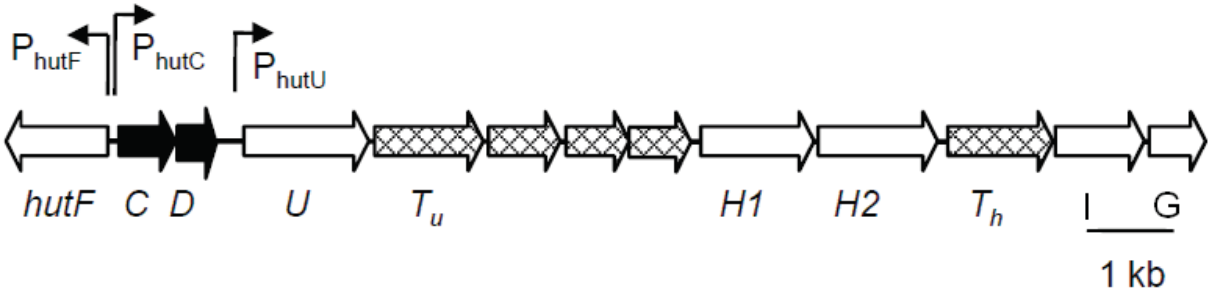

Figure 1.2. A simplified genetic organization of a *Pseudomonas hut* operon. Metabolic and regulator genes are shown by white and black arrows, respectively. Crosshatched arrows indicate genes encoding transporters described in this report. The *hut* genes are arranged in two transcriptional units and the transcriptional orientation is indicated by arrows. (Zhang and Rainey 2007)

1.3 Objectives of this study

This work focuses on the genotypic and phenotypic characterization of 230 *Pseudomonas* strains, which were isolated from the phyllosphere of sugar beets: 164 strains from sugar beets grown in Oxford (UK) (Haubold and Rainey 1996) and 66 strains from Auckland (New Zealand). Part of the 164 strains (108 isolates) have been subjected to a previous multi-locus enzyme electrophoresis (MLEE) analysis wherein details of the sampling were provided (Haubold and Rainey 1996). The objectives of this study are:

1> To examine the phenotypic variation of the two populations of plant-associated *Pseudomonas*, in terms of their ability to utilize histidine and urocanate as the sole source of carbon and nitrogen.

2> To elucidate the genetic basis of the phenotypic variation, specifically testing the hypothesis that variance in transport systems, and not in

metabolic genes, explains polymorphism of histidine and urocanate utilization in plant-associated *Pseudomonas*.

3> To characterize the genetic relatedness of the two populations of plant-associated *Pseudomonas*, using multi-locus sequence analysis (MLSA) of three genes (*gapA, gltA and acnB*). A possible correlation between genotype and phenotype is analyzed and discussed.

Chapter 2: Materials and Methods

2.1 Materials

2.1.1 Bacterial strains, media and growth conditions

Unless otherwise specified, all chemicals in this section were obtained from BDH, and all equipment from BioLab. Bacteria were cultured in LB (Bertani 1951): 10 g NaCl, 10 g peptone, 5 g yeast extract L^{-1}, or minimal M9 medium (Sambrook et al. 1989): 34 g Na_2HPO_4, 15 g KH_2PO_4, 2.5 g NaCl, 5 g 1.8M NH_4Cl, 15 mg 1 M $CaCl_2$.6H2O, 1 ml 1 M $MgSO_4.7H_2O$, 10 ml 20 % ($^w/_v$) glucose L^{-1}. Where indicated, *Pseudomonas* strains were also cultivated in minimal-M9 medium (Sambrook et al. 1989) supplemented with glucose (0.4% or 22.2 mM) and NH4Cl (1 mg ml^{-1} or 18.7 mM). When histidine or urocanate were used as sole carbon and nitrogen sources, they replaced the glucose and ammonia of the M9 medium and were added at a final concentration of 15 mM. When necessary, antibiotics were included at the following concentrations: tetracycline (Tc), 10 µg ml^{-1}; kanamycin (Km), 50 µg ml^{-1}; spectinomycin (Sp), 100 µg ml^{-1}; nitrofurantoin (Nf), 100 µg ml^{-1}.

Where appropriate, bacteriological agar (H.J. Langdon) was added to a concentration of 1.5 % ($^w/_v$). Overnight cultures were grown for overnight with shaking at 150 rpm unless specified, in 30 ml plastic tubes containing 5 ml LB. *Pseudomonas* strains were grown at 28°C while *E. coli* strains were grown at 37°C.

Growth kinetics of all *Pseudomonas* and the derived mutant strains were determined in microtiter plates using a VersaMax microtiter plate reader with SOFTmax PRO software (Molecular Devices). To ensure that all bacteria were physiologically equivalent, strains were inoculated from cells stored in a −80°C freezer. They were first grown in LB broth (24 hr) and then subcultured once in M9 broth (24 hr) before use in assay conditions. Absorbance at the wavelength of 450 nm was determined every 5 min over a period of 48 hr.

Bacterial strains used are listed below in Table 2.1 All strains were stored indefinitely at -80°C in 45 % ($^{v}/_{v}$) glycerol saline.

Table 2.1: Designations and characteristics of bacterial strains used. The phenotypic characteristics of histidine and urocanate were indicated. Sampling time referred to two periods of *Pseudomonas* strain isolations from sugar beet plants, indicated as "1" or "2". Note that *P. fluorescens* SBW25 was not included during strain isolation, therefore "N/A" was given. Some isolates that could not recover from the cryogenic storage and subjected to this study were labeled as "No data". Each isolated strain was also named as its origin of isolation, as described in 2.1.2.

Strain	Sampling time	Genotypes or relevant His/Uro characteristics	Source or alternative names
Pseudomonas species			
P. fluorescens SBW25	N/A	Wild-type strain isolated from sugar beet	Thompson et al. (1995)
U100	1	Environmental strain isolated from sugar beet	823a1
U101	1	Environmental strain isolated from sugar beet	823a2
U102	1	Environmental strain isolated from sugar beet	815a1
U103	1	Environmental strain isolated from sugar beet	815a1
U104	1	Environmental strain isolated from sugar beet	815b1
U105	1	Environmental strain isolated from sugar beet	815b2
U106	1	Environmental strain isolated from sugar beet	813a1
U107	1	Environmental strain isolated from sugar beet	813a2
U108	1	Environmental strain isolated from sugar beet	311a1
U109	1	Environmental strain isolated from sugar beet	311a2
U110	1	Environmental strain isolated from sugar beet	821a1
U111	1	Environmental strain isolated from sugar beet	821a2
U112	1	Environmental strain isolated from sugar beet	831b1
U113	1	Environmental strain isolated from sugar beet	831b2
U114	1	Environmental strain isolated from sugar beet	425a1
U115	1	Environmental strain isolated from sugar beet	425a2
U116	1	Environmental strain isolated from sugar beet	413b1
U117	1	Environmental strain isolated from sugar beet	413b2
U118	1	Environmental strain isolated from sugar beet	315a1
U119	1	Environmental strain isolated from sugar beet	315a2
U120	1	Environmental strain isolated from sugar beet	811b1
U121	1	Environmental strain isolated from sugar beet	811b2
U122	1	Environmental strain isolated from sugar beet	421b1
U123	1	Environmental strain isolated from sugar beet	421b2
U124	1	Environmental strain isolated from sugar beet	335a1
U125	1	Environmental strain isolated from sugar beet	335a2
U126	1	Environmental strain isolated from sugar beet	311b1
U127	1	Environmental strain isolated from sugar beet	311b2
U128	1	Environmental strain isolated from sugar beet	331b1
U129	1	Environmental strain isolated from sugar beet	331b2
U130	1	Environmental strain isolated from sugar beet	423a1

U131	1	Environmental strain isolated from sugar beet	423a2
U132	1	Environmental strain isolated from sugar beet	435a1
U133	1	Environmental strain isolated from sugar beet	435a2
U134	1	Environmental strain isolated from sugar beet	431a2
U135	1	Environmental strain isolated from sugar beet	431a1
U136	1	Environmental strain isolated from sugar beet	433b1
U137	1	Environmental strain isolated from sugar beet	433b2
U138	1	Environmental strain isolated from sugar beet	431b1
U139	1	Environmental strain isolated from sugar beet	431b2
U140	1	Environmental strain isolated from sugar beet	425b1
U141	1	Environmental strain isolated from sugar beet	425b2
U142	1	Environmental strain isolated from sugar beet	421a1
U143	1	Environmental strain isolated from sugar beet	421a2
U144	1	Environmental strain isolated from sugar beet	335b2
U145	1	Environmental strain isolated from sugar beet	335b1
U146	1	Environmental strain isolated from sugar beet	321a1
U147	1	Environmental strain isolated from sugar beet	321a2
U148	1	Environmental strain isolated from sugar beet	423b1
U149	1	Environmental strain isolated from sugar beet	423b2
U150	1	Environmental strain isolated from sugar beet	333a1
U151	1	Environmental strain isolated from sugar beet	333a2
U152	1	Environmental strain isolated from sugar beet	415b1
U153	1	Environmental strain isolated from sugar beet	415b2
U154	1	Environmental strain isolated from sugar beet	813a1
U155	1	Environmental strain isolated from sugar beet	831a2
U156	1	Environmental strain isolated from sugar beet	325a1
U157	1	Environmental strain isolated from sugar beet	325a2
U158	1	Environmental strain isolated from sugar beet	315b1
U159	1	Environmental strain isolated from sugar beet	315b2
U160	1	Environmental strain isolated from sugar beet	323b1
U161	1	Environmental strain isolated from sugar beet	323b2
U162	1	Environmental strain isolated from sugar beet	435b1
U163	1	Environmental strain isolated from sugar beet	435b2
U164	1	Environmental strain isolated from sugar beet	333b1
U165	1	Environmental strain isolated from sugar beet	333b2
U166	1	Environmental strain isolated from sugar beet	325b1
U167	1	Environmental strain isolated from sugar beet	325b2
U168	1	Environmental strain isolated from sugar beet	833a1
U169	1	Environmental strain isolated from sugar beet	833a2
U170	1	Environmental strain isolated from sugar beet	413a1
U171	1	Environmental strain isolated from sugar beet	413a2
U172	1	Environmental strain isolated from sugar beet	331a1
U173	1	Environmental strain isolated from sugar beet	331a2
U174	1	Environmental strain isolated from sugar beet	825a1
U175	1	Environmental strain isolated from sugar beet	825a2
U176	1	Environmental strain isolated from sugar beet	323a2

U177	1	Environmental strain isolated from sugar beet	323a1
U178	1	Environmental strain isolated from sugar beet	415a1
U179	1	Environmental strain isolated from sugar beet	415a2
U180	1	Environmental strain isolated from sugar beet	411b1
U181	1	Environmental strain isolated from sugar beet	411b2
U182	1	Environmental strain isolated from sugar beet	313b1
U183	1	Environmental strain isolated from sugar beet	313b2
U184	1	Environmental strain isolated from sugar beet	313a1
U185	1	Environmental strain isolated from sugar beet	313a2
U186	1	Environmental strain isolated from sugar beet	835a1
U187	1	Environmental strain isolated from sugar beet	835a2
U188	1	Environmental strain isolated from sugar beet	825b1
U189	1	Environmental strain isolated from sugar beet	825b2
U190	1	Environmental strain isolated from sugar beet	833b1
U191	1	Environmental strain isolated from sugar beet	833b2
U192	1	Environmental strain isolated from sugar beet	835b1
U193	1	Environmental strain isolated from sugar beet	835b2
U194	1	Environmental strain isolated from sugar beet	813b1
U195	1	Environmental strain isolated from sugar beet	813b2
U196	1	Environmental strain isolated from sugar beet	823b1
U197	1	Environmental strain isolated from sugar beet	823b2
U198	1	Environmental strain isolated from sugar beet	433a2
U199	1	Environmental strain isolated from sugar beet	433a1
U200	1	Environmental strain isolated from sugar beet	821b1
U201	1	Environmental strain isolated from sugar beet	821b2
U202	1	Environmental strain isolated from sugar beet	321b1
U203	1	Environmental strain isolated from sugar beet	321b2
U204	1	Environmental strain isolated from sugar beet	811a1
U205	1	Environmental strain isolated from sugar beet	811a2
U206	1	Environmental strain isolated from sugar beet	411a1
U207	1	Environmental strain isolated from sugar beet	411a2
U208	2	Environmental strain isolated from sugar beet	413a2
U209	2	Environmental strain isolated from sugar beet	425b1
U210	2	Environmental strain isolated from sugar beet	411a2
U211	2	Environmental strain isolated from sugar beet	435a1
U212	2	Environmental strain isolated from sugar beet	431b2
U213	2	Environmental strain isolated from sugar beet	333b1
U214	2	Environmental strain isolated from sugar beet	323a2
U215	2	Environmental strain isolated from sugar beet	325a1
U216	2	Environmental strain isolated from sugar beet	311b2
U217	2	Environmental strain isolated from sugar beet	315b1
U218	2	Environmental strain isolated from sugar beet	335a2
U219	2	Environmental strain isolated from sugar beet	313a1
U220	2	Environmental strain isolated from sugar beet	413b1
U221	2	Environmental strain isolated from sugar beet	425b2
U222	2	Environmental strain isolated from sugar beet	425a1

U223	2	Environmental strain isolated from sugar beet	435a2
U224	2	Environmental strain isolated from sugar beet	433a1
U225	2	Environmental strain isolated from sugar beet	333b2
U226	2	Environmental strain isolated from sugar beet	323b1
U227	2	Environmental strain isolated from sugar beet	325a2
U228	2	Environmental strain isolated from sugar beet	331a1
U229	2	Environmental strain isolated from sugar beet	315b2
U230	2	Environmental strain isolated from sugar beet	335b1
U231	2	Environmental strain isolated from sugar beet	313a2
U232	2	Environmental strain isolated from sugar beet	413b2
U233	2	Environmental strain isolated from sugar beet	415a1
U234	2	Environmental strain isolated from sugar beet	425a2
U235	2	Environmental strain isolated from sugar beet	435b1
U236	2	Environmental strain isolated from sugar beet	433a2
U237	2	Environmental strain isolated from sugar beet	431a1
U238	2	Environmental strain isolated from sugar beet	323b2
U239	2	Environmental strain isolated from sugar beet	325b1
U240	2	Environmental strain isolated from sugar beet	331a2
U241	2	Environmental strain isolated from sugar beet	311a1
U242	2	Environmental strain isolated from sugar beet	335b2
U243	2	Environmental strain isolated from sugar beet	313b1
U244	2	Environmental strain isolated from sugar beet	421a1
U245	2	Environmental strain isolated from sugar beet	415a2
U246	2	Environmental strain isolated from sugar beet	415b1
U247	2	Environmental strain isolated from sugar beet	435b2
U248	2	Environmental strain isolated from sugar beet	433b1
U249	2	Environmental strain isolated from sugar beet	431a2
U250	2	Environmental strain isolated from sugar beet	333a1
U251	2	Environmental strain isolated from sugar beet	325b2
U252	2	Environmental strain isolated from sugar beet	331b1
U253	2	Environmental strain isolated from sugar beet	311a2
U254	2	Environmental strain isolated from sugar beet	315a1
U255	2	Environmental strain isolated from sugar beet	313b2
U256	2	Environmental strain isolated from sugar beet	421a2
U257	2	Environmental strain isolated from sugar beet	413a1
U258	2	Environmental strain isolated from sugar beet	415b2
U259	2	Environmental strain isolated from sugar beet	411a1
U260	2	Environmental strain isolated from sugar beet	433b2
U261	2	Environmental strain isolated from sugar beet	431b1
U262	2	Environmental strain isolated from sugar beet	333a2
U263	2	Environmental strain isolated from sugar beet	323a1
U264	2	Environmental strain isolated from sugar beet	331b2
U265	2	Environmental strain isolated from sugar beet	311b1
U266	2	Environmental strain isolated from sugar beet	315a2
U267	2	Environmental strain isolated from sugar beet	335a1
U268	2	Environmental strain isolated from sugar beet	833b1

U269	2	Environmental strain isolated from sugar beet	833b2
X111a1	1	Environmental strain isolated from sugar beet	X.-X. Zhang
X111a2	1	Environmental strain isolated from sugar beet	X.-X. Zhang
X111b1	1	Environmental strain isolated from sugar beet	X.-X. Zhang
X111b2	1	Environmental strain isolated from sugar beet	X.-X. Zhang
X113a1	1	Environmental strain isolated from sugar beet	X.-X. Zhang
X113a2	1	Environmental strain isolated from sugar beet	X.-X. Zhang
X113b1	1	Environmental strain isolated from sugar beet	X.-X. Zhang
X113b2	1	Environmental strain isolated from sugar beet	X.-X. Zhang
X115a1	1	Environmental strain isolated from sugar beet	X.-X. Zhang
X115a2	1	Environmental strain isolated from sugar beet	X.-X. Zhang
X115b1	1	Environmental strain isolated from sugar beet	X.-X. Zhang
X115b2	1	Environmental strain isolated from sugar beet	X.-X. Zhang
X121a1	1	Environmental strain isolated from sugar beet	X.-X. Zhang
X121a2	1	Environmental strain isolated from sugar beet	X.-X. Zhang
X121b1	1	Environmental strain isolated from sugar beet	X.-X. Zhang
X121b2	1	Environmental strain isolated from sugar beet	X.-X. Zhang
X123a1	1	Environmental strain isolated from sugar beet	X.-X. Zhang
X123a2	1	Environmental strain isolated from sugar beet	X.-X. Zhang
X123b1	1	Environmental strain isolated from sugar beet	X.-X. Zhang
X123b2	1	Environmental strain isolated from sugar beet	X.-X. Zhang
X125a1	1	Environmental strain isolated from sugar beet	X.-X. Zhang
X125a2	1	Environmental strain isolated from sugar beet	X.-X. Zhang
X125b1	1	Environmental strain isolated from sugar beet	X.-X. Zhang
X125b2	1	Environmental strain isolated from sugar beet	X.-X. Zhang
X131a1	1	Environmental strain isolated from sugar beet	X.-X. Zhang
X131a2	1	Environmental strain isolated from sugar beet	X.-X. Zhang
X131b1	1	Environmental strain isolated from sugar beet	X.-X. Zhang
X131b2	1	Environmental strain isolated from sugar beet	X.-X. Zhang
X133a1	1	Environmental strain isolated from sugar beet	X.-X. Zhang
X133a2	1	Environmental strain isolated from sugar beet	X.-X. Zhang
X133b1	1	Environmental strain isolated from sugar beet	X.-X. Zhang
X133b2	1	Environmental strain isolated from sugar beet	X.-X. Zhang
X135a1	1	Environmental strain isolated from sugar beet	X.-X. Zhang
X135a2	1	Environmental strain isolated from sugar beet	X.-X. Zhang
X135b1	1	Environmental strain isolated from sugar beet	X.-X. Zhang
X135b2	1	Environmental strain isolated from sugar beet	X.-X. Zhang
X141a1	1	Environmental strain isolated from sugar beet	X.-X. Zhang
X141a2	1	Environmental strain isolated from sugar beet	X.-X. Zhang
X141b1	1	Environmental strain isolated from sugar beet	X.-X. Zhang
X141b2	1	Environmental strain isolated from sugar beet	X.-X. Zhang
X143a1	1	Environmental strain isolated from sugar beet	X.-X. Zhang
X143a2	1	Environmental strain isolated from sugar beet	X.-X. Zhang
X143b1	1	Environmental strain isolated from sugar beet	X.-X. Zhang
X143b2	1	Environmental strain isolated from sugar beet	X.-X. Zhang
X145a1	1	Environmental strain isolated from sugar beet	X.-X. Zhang

X145a2	1	Environmental strain isolated from sugar beet	X.-X. Zhang
X145b1	1	Environmental strain isolated from sugar beet	X.-X. Zhang
X145b2	1	Environmental strain isolated from sugar beet	X.-X. Zhang
X151a1	1	Environmental strain isolated from sugar beet	X.-X. Zhang
X151a2	1	Environmental strain isolated from sugar beet	X.-X. Zhang
X151b1	1	Environmental strain isolated from sugar beet	X.-X. Zhang
X151b2	1	Environmental strain isolated from sugar beet	X.-X. Zhang
X153a1	1	Environmental strain isolated from sugar beet	X.-X. Zhang
X153a2	1	Environmental strain isolated from sugar beet	X.-X. Zhang
X153b1	1	Environmental strain isolated from sugar beet	X.-X. Zhang
X153b2	1	Environmental strain isolated from sugar beet	X.-X. Zhang
X155a1	1	Environmental strain isolated from sugar beet	X.-X. Zhang
X155a2	1	Environmental strain isolated from sugar beet	X.-X. Zhang
X155b1	1	Environmental strain isolated from sugar beet	X.-X. Zhang
X155b2	1	Environmental strain isolated from sugar beet	X.-X. Zhang
12163	1	Environmental strain isolated from sugar beet	X.-X. Zhang
xx1163	1	Environmental strain isolated from sugar beet	X.-X. Zhang
15393 v1	1	Environmental strain isolated from sugar beet	X.-X. Zhang
15393v2	1	Environmental strain isolated from sugar beet	X.-X. Zhang
x151a3	1	Environmental strain isolated from sugar beet	X.-X. Zhang
x141b3 spreader	1	Environmental strain isolated from sugar beet	X.-X. Zhang
U118Th		vector contains histidine transporter	This study
U119Th		vector contains histidine transporter	This study
U121Th		vector contains histidine transporter	This study
U128Th		vector contains histidine transporter	This study
U128H2		chromosome integrated with functional histidase	This study
U128ThH2		dual complementations of histidine transporter and funcitonal histidase	This study
U134Th		vector contains histidine transporter	This study
U136Th		vector contains histidine transporter	This study
U143Th		vector contains histidine transporter	This study
U148Th		vector contains histidine transporter	This study
U158Th		vector contains histidine transporter	This study
U159Th		vector contains histidine transporter	This study
U161Th		vector contains histidine transporter	This study
U165Tu		vector contains urocanate transporter	This study
U166Tu		vector contains urocanate transporter	This study
U172Th		vector contains histidine transporter	This study
U173Th		vector contains histidine transporter	This study
U174Th		vector contains histidine transporter	This study
U176Th		vector contains histidine transporter	This study
U182Th		, vector contains histidine transporter	This study
U184Th		vector contains histidine transporter	This study
U191Th		vector contains histidine transporter	This study
U197Th		vector contains histidine transporter	This study
U203Th		vector contains histidine transporter	This study

U212		vector contains urocanate transporter	This study
U216Th		vector contains histidine transporter	This study
U249		vector contains urocanate transporter	This study
U256		vector contains urocanate transporter	This study
U261		vector contains urocanate transporter	This study
U265Th		vector contains histidine transporter	This study
X111a2		vector contains urocanate transporter	This study
X111b1		vector contains urocanate transporter	This study
X111b2		vector contains urocanate transporter	This study
X113a1		vector contains urocanate transporter	This study
X113b1		vector contains urocanate transporter	This study
X123a2		vector contains urocanate transporter	This study
X131b1		vector contains urocanate transporter	This study
X141b1		vector contains urocanate transporter	This study
X143a1		vector contains urocanate transporter	This study
X143a2		vector contains urocanate transporter	This study
X151b1		vector contains urocanate transporter	This study
Escherichia coli			
DH5α-λpir		λpir	Invitrogen
TOP10		*hutH2*	Invitrogen

2.1.2 Sampling and naming of *Pseudomonas* isolates

The sampling details of the *Pseudomonas* isolated from Oxford were described previously (Haubold and Rainey 1996). Additionally, an extra 66 *Pseudomonas* isolates were sampled using the same sampling method but from Auckland. All strains were showing in Table 2.1. Each strain was assigned a code which indicating the origin of isolation: plot (1, 3, 4, or 8), plant (1, 2, 3, 4, or 5), leaf (1, senescent; 3, mature; 5, immature), and replicate leaf (a or b). The Auckland isolates were labelled “X” to distinguish those from Oxford populations. For instance, strain X131b1 identifies Auckland isolate 1 from senescent (1) leaf “b”, from plant 3, from plot 1. Strain 835a1 indicates Oxford isolate 1 from immature (5) leaf “a”, from plant 3, from plot 8. For simplicity, Oxford strains were also labelled as numerical numbers starting from U100 to U269 in Table 2.1, and this study is referring this naming system.

2.1.3 Plasmids

Table 2.2: Designations and characteristics of plasmids used.

Plasmid Strains	Genotypes and relevant characteristics	Source or reference
pME6010-H2	*hutH2* construct for complementation, Tc^R	X.-X. Zhang
pME6010-Th	*hutTh* construct for complementation, Tc^R	X.-X. Zhang
pME3010-Tu	*hutTu* construct for complementation, Tc^R	X.-X. Zhang
pRK2013	Km^R, IncP4, *tra*, *mob*; mobilization plasmid used as a helper for tri-parental mating	(Figurski and Helinski 1979)
pUIC3	Tc^R, *mob*, *oriR6K*, *bla*, Δpromoter-*lacZY*	Rainey (1999)
pUIC3_H2	pUIC3::*hutH2*	X.-X. Zhang
mini-Tn7-LAC	LacZ, Gm^R, Km^R	(Choi et al. 2005)
pCR8/GW/TOPO	SpeR, pUC *ori*; 2.8 kb sequencing plasmid	Invitrogen

2.1.4 Primers

Primers were synthesized by Invitrogen or Integrated DNA Technologies (IDT), and were resuspended in deionised water to a concentration of 100 pmol μl^{-1}, and were stored at -20°C. Primers were used at a final working concentration of 10 pmol μl^{-1}.

Table 2.3: Primers used in this study.

Name	Sequence (5' to 3')	Target
hutTuF	TCGAGGATTGAACAACATGGCTGCAAATG	*hutTu* (SBW25)
hutTuR	GAAGATCTGCCCTGTCCACGTCCCATCA	*hutTu* (SBW25)
hutThF	TCGAGGAAGGACGAGAAATGCAACAGC	*hutTh* (SBW25)
hutThR	CGGGATCCAAAGCGTTTTCATCAACG	*hutTh* (SBW25)
hutH2F1	ATCGMCGMCAGCGTNGCCTG	*hutH2* (all *Pseudomonas*)
hutH2F2	GGYTTYGGCCTGCTSGCYTCGAC	*hutH2* (all *Pseudomonas)*
hutH2R1	TGSGTRCCRTTGAGCAGBGCCA	*hutH2* (all *Pseudomonas)*
hutH2R2	CCRCGCARBGCRTABGCGGTGGA	*hutH2* (all *Pseudomonas)*
hutIR	TCGAAYTCRCCRCTGCGRTTGCC	*hutI* (all *Pseudomonas)*
hutUF	GGVATGGTSATCGTCTGYGACGG	*hutU* (all *Pseudomonas)*
Tn7R-109	CAGCATAACTGGACTGATTTCAG	Tn7 vector
SBW25-GlmS	CACCAAAGCTTTCACCACCCAA	*GlmS* (SBW25)
U128-H2F	TGAAACCGGAGTTGACCCCGC	*hutH2* (U128)
U128-H2R	TGAGGCCGGCGATTTTCAGC	*hutH2* (U128)
gapFSP	CGCAAYCCSGCSGAVCTGCC	*gapA* (all

		Pseudomonas)
gapRSP	GTGTGRTTGGCRTCGAARATCGA	*gapA* (all *Pseudomonas*)
gltFSP	GAAAACTTCCTSCACATGATGTTC	*gltA* (all *Pseudomonas*)
gltRS	TAGAAGTCSACGTTCGGGTA	*gltA* (all *Pseudomonas*)
gltRP	GTMCGYGCCAGGGCGAAGAT	*gltA* (all *Pseudomonas*)
acnFP	CGGTRCTSTGGTTCTTCGGCGACGAC	*acnB* (all *Pseudomonas*)
acnFS	CCGATCTTCTAYAACACCATGGAAG	*acnB* (all *Pseudomonas*)
acnRP	TTCTTCTCKACGGTCAGCAGGCC	*acnB* (all *Pseudomonas*)
acnRS	CCAGGTCRCGCAGGGTGATGCC	*acnB* (all *Pseudomonas*)

2.2 Methods

2.2.1 Polymerase chain reaction (PCR)

Polymerase chain reactions were carried out using a CG1-96 Thermal Cycler (Corbett Life Sciences). A standard 25 µl reaction contained: 2.5 µl 10 *x* PCR buffer, 0.5 µl 10 mM dNTP mix, 0.8 µl 50 mM MgCl2, 0.2 µl Taq polymerase, 1 µl of each 10 pmol µl-1 primer and 30-100 ng template DNA, made up to 25 µl with deionised water. Following an initial template denaturation step of 3 minutes at 94°C, amplification was performed by 30 cycles of denaturation for 15 seconds at 94°C, annealing for 30 seconds at 55-62°C, and strand extension for 1 minute per kilobase (kb) of target DNA at 72°C. If no PCR products or non-specific PCR products were detected at initial annealing temperatures, empirical tests were performed to find optimal annealing temperatures for the primers. In cases where PCR products were to be used for cloning into pCR8/GW/TOPO, a final extension step of 10 minutes at 72°C was performed before the sample was cooled to 4°C indefinitely. If no PCR products or non-specific PCR products were detected at initial annealing temperatures, empirical tests were performed to find optimal annealing temperatures for the primers.

2.2.2 Cloning and transformation techniques

2.2.2.1 Plasmid purification, digestion and ligation

Cloning was carried out under sterile conditions according to standard molecular biology techniques (Sambrook et al. 1989). Plasmid DNA was extracted from overnight bacterial cultures using a QIAprep® Spin Miniprep Kit (Qiagen), and stored in 50 µl aliquots at -20°C. The obtained DNA was digested with restriction enzymes (Invitrogen) in the appropriate React buffers at 37ºC for at least 2 hours or overnight. Following digestion of the extracted plasmid and desired insert with the appropriate restriction enzyme(s), ligation reactions were carried out by overnight incubation at 4°C with T4 DNA ligase in a final volume of 10 µl, containing 2 µl 5 x ligase buffer, 4.5 µl insert and 3 µl vector. Alternatively, freshly amplified PCR products were cloned directly into pCR8/GW/TOPO using the TOPO® TA cloning protocol. Reactions were set up according to manufacturer's instructions: 4 µl fresh PCR product, 1 µl salt solution and 1 µl vector were gently mixed and incubated at room temperature (23-25°C) for 10 minutes, before storing at -20°C.

2.2.2.2 Manufacture of *E. coli* chemically competent cells

E. coli DH5α-*λpir* chemically competent cells were produced from overnight cultures grown to mid-log phase in 200 ml LB media. Four 50 ml aliquots of cell culture were pelleted in Falcon tubes (500 x g, 10 minutes). Pellets were re-suspended in 1 ml ice-cold TBFI, and subsequently combined. 10 ml further TBFI was added and the resulting mixture incubated on ice for 60 minutes. Cells were then pelleted (500 x g, 10 minutes) and re-suspended in 4 ml ice-cold TBFII. 50 µl aliquots of the newly competent cells were snap frozen and stored at -80°C until required.

2.2.2.3 Electrophoretion of *P. fluorescens* and *E.coli* chemically competent cells

2 µl of plasmid DNA or ligation product was added to 50 µl of electrocompetent cells that had been thawed on ice. The cells were placed between 0.1 cm electrodes of a pre-chilled gapped Gene Pulser® cuvette (Bio-Rad) and

electroporated using Electroporator 2510 (Eppendorf) at 1.8 kV. 800 µl of SOC medium (2% Bacto Tryptone, 10 mM $MgCl_2$, 0.5% Yeast Extract, 10 mM $MgSO_4$, 20 mM Glucose, 10 mM NaCl and 2.5 mM KCl) was immediately added and the electroporated cells were transferred to a 1.5 ml sterile eppendorf tube. The cells were incubated at 37ºC with shaking at 180 rpm for 1 hour. The culture was spread onto LB plates containing the appropriate antibiotic and incubated at 37ºC overnight. After incubation, colonies of transformants were inoculated into 5 ml of LB containing the appropriate antibiotic and grown 37ºC with shaking at 180 rpm overnight. Plasmid DNA was isolated from these cultures.

2.2.3 Agarose gel electrophoresis

DNA fragments were separated on 1% agarose gels in 1x TBE buffer (UltraPure™,Invitrogen) containing 1x SYBR Safe™ DNA gel stain (Invitrogen). Samples were mixed with 6x DNA loading dye (Fermentas) at the ratio of 1:5 prior to loading onto the gel. Gels were run at 140 volts for 30-60 minutes. Lambda DNA/EcoRI+HindIII marker (Fermentas) was also loaded to estimate the size of DNA fragments. Visualization of DNA was undertaken using UV light generated from a High Performance Transilluminators (UVP, LLC) and gels were photographed using DigiDoc-It™ Imaging System with Doc-It LS Analysis Software (UVP, LLC).

2.2.4 DNA sequencing

Plasmid DNA and PCR products were prepared for sequencing using a QIAprep® Spin Miniprep Kit and a QIAquick® PCR Purification Kit or QIAquick® Gel Extraction Kit (Qiagen), respectively. Purified DNA samples were sent to Macrogen (Seoul, Korea) for Sanger sequencing and analysis. Sequence traces were analyzed using FinchTV version 1.4.0 (Geospiza) and aligned using Geneious version Pro 4.7.6 (Biomatters).

2.2.5 Tri-Parental conjugation

Overnight cell cultures of the *E. coli* donor, *E. coli* DH5α containing the helper

plasmid pRK2013 and *P. fluorescens* recipient strains were grown in LB containing appropriate antibiotics. 1 ml of the recipient culture was heatshocked for 20 minutes at 45°C before pelleting (13,000 x g, 1 minute). 300 µl of the donor and helper culture were also pelleted (13,000 x g, 1 minute). All pellets were re-suspended in 200 µl LB, and subsequently mixed thoroughly. Cells were pelleted once more (13,000 x g, 1 minute) prior to re-suspension in 30 µl LB. The resulting concentrated resuspension was gently dropped and spread onto the centre of a pre-warmed LB agar plate, allowed to dry and incubated for 24 hours at 28°C. After incubation, the inoculum was removed and re-suspended in 1 ml fresh LB. A dilution series was prepared in sterile water and plated onto LB agar plates containing NF (to select against *E. coli*) and Km or Tc (to select for the donor plasmid), as specified. After 48 hours growth at 28°C, individual colonies were selected and purified by re-streaking, and stored at -80°C.

2.2.6 Computational Analysis

Unless stated, the phylogenetic analysis part of this report were using SplitsTree4 version 4.10 (www.splitstree.org) and ClonalFrame version 1.1 (http://bacteria.stats.ox.ac.uk). The graphs were constructed by using SigmaPlot version 7.0 (SPSS Inc.).

Chapter 3: Results

3.1 Histidine and urocanate utilization in plant-associated *Pseudomonas*

A total of 230 leaf-colonizing *Pseudomonas* strains were subjected to phenotypic analysis whereby their ability to utilize histidine and urocanate was assessed. All *Pseudomonas* strains were isolated from the same cultivar of sugar beet (*Beta vulgaris* var. Amethyst) plants grown in two geographic locations: 164 strains in Oxford (UK) and 66 strains in Auckland (NZ). Growth (absorbance at the wavelength of 450 nm) was measured using a microtiter plate reader over a period of 48 hrs at 28°C. (See Materials and Methods section). Because bacterial growth is dynamic and many factors including mutations and contaminations from the environment can "false" the absorbance readings, in this thesis, no growth refers to the absence of exponential growth phase and the maximal absorbance (*A450*) less than 0.4. Results are summarized in Table 3.1, and details of the results are listed in Table 3.2 and 3.3.

Table 3.1. The utilization of histidine or urocanate as the sole carbon and nitrogen sources for Oxford and Auckland *Pseudomonas.* Growth (+): OD450 >0.4; no growth (-): OD450 <0.4. The numbers in the brackets represent the percentages of strains that contribute to the population.

Phenotypes		**Number of strains**		
Histidine	Urocanate	Oxford	Auckland	Total
+	+	127 (77%)	23 (33%)	150 (65.2%)
+	-	8 (5%)	17 (30%)	25 (10.9%)
-	+	29 (18%)	0	29 (12.5%)
-	-	0	26 (37%)	26 (11.3%)

Table 3.2. The utilization of histidine or urocanate as the sole carbon and nitrogen sources for Oxford (UK) *Pseudomonas*

Phenotypes	Number of isolates	Isolate Identifications
His^+, Uro^+	127	U102, U103, U104, U106, U107, U108, U109, U110, U111, U112, U113, U114, U115, U116, U117, U120, U122, U123, U124, U125, U129, U130, U131 U132, U135, U137, U138, U139, U140, U141, U142, U144, U145, U146, U147, U149, U150, U151, U152, U153, U154, U155, U156, U157, U164, U167, U168, U169, U170, U171, U174, U175, U178, U179, U180, U183, U185, U186, U187, U188, U189, U190, U192, U193, U195, U196, U198, U199, U200, U201, U202, U204, U205, U207, U208, U209, U210, U211, U213, U214, U215, U217, U219, U220, U221, U222, U223, U224, U225, U226, U267, U227, U228, U229, U230, U231, U232, U233, U234, U235, U236, U237, U238, U239, U240, U241, U243, U244, U245, U246, U247, U248, U250, U251, U252, U253, U254, U255, U257, U258, U259, U260, U262, U263, U266, U268, U269
His^+, Uro^-	8	U165, U166, U181, U206, U212, U249, U256, U261
His^-, Uro^+	29	U100, U101, U105, U118, U119, U121, U126, U127, U128, U134, U136, U143, U148, U158, U159, U160, U161, U172, U173, U176, U177, U182, U184, U191, U194, U197, U203, U216, U265,
His^-, Uro^-	0	

Table 3.3. The utilization of histidine or urocanate as the sole carbon and nitrogen sources for Auckland (New Zealand) *Pseudomonas*

Phenotypes	Number of isolates	Isolate Identifications
His^+, Uro^+	23	X121a1, X121a2, X123a1, X123b1, X125a1, X125a2, X125b1, X125b2, X131b2, X135a1, X135a2, X135b1, 135b2, X141a1, X145a1, X145a2, X145b1, X145b2, X151a1, X151a2, X151a3, X155a1, X155b2,
His^+, Uro^-	17	X111a2, X111b1, X111b2, X111b3, X113a1, X115a2, X115b2, X123a2, X123b2, X141a2, X141b2, X143a1, X143a2, X143b1, X143b2, X151b1, X151b2,
His^-, Uro^+	0	
His^-, Uro^-	26	X111a1, X113a2, X113b1, X113b2, X115a1, X115b1, X121b1, X121b2, 121b3, X131a1, X131a2, X131b1, X133a1, X133a2, X133b1, X133b2, X141b1, X141b3, X153a1, X153a2, X153b1, X153b2, X155a2, X155b1, 153a3V1, 153a3V2,

As shown in Table 3.1, the two *Pseudomonas* populations display a great of phenotypic diversity. Most isolates (65%) are His^+, Uro^+ (capable of utilizing both histidine and urocanate as growth substrates), and approximately 11% of the isolates are His^-, Uro^- (Table 3.1). Interestingly, the remaining isolates were the phenotypes that could utilize either histidine, but not urocanate (His^+, Uro^-; 11%), or vice versa (His^-, Uro^+; 13%). Of particular interest is that, the His^-, Uro^+ strains are prevalent in the Oxford population (18%), but none in the Auckland population; meanwhile, His^+, Uro^- strains are more commonly found in the Auckland population (30% in Auckland vs. 5% in Oxford).

3.2 Phenotypic diversity of histidine and urocanate utilization is attributable to variation in transporters

Given that both histidine and urocanate are degraded by the same catabolic pathway (Fig. 1.1), the finding that a lot of *Pseudomonas* isolates (~ 24%) use one substrate but not the other is of interest (refer to the His^+ Uro^- and His^- Uro^+ strains in Table 3.2 and 3.3). If one strain can grow on histidine, it must harbour all the enzymes required for the bacterium to grow on urocanate; the fact that it can't grow on urocanate (His^+ Uro^-) suggested that a functional transporter for urocanate is missing. Similarly for strains of His^- Uro^+, it is predicted that they may lack a functional histidine transporter and/or a functional histidase (*hutH*), which converts histidine to urocanate. Additionally, preliminary *in silico* analysis of 17 genome-sequenced *Pseudomonas hut* locus showed highly conservations of major metabolite genes but poorly on the remaining parts including transporter genes. This led to a hypothesis that diversity of histidine and urocanate utilization is attributable to variation in transporters, and less likely in catabolic genes.

3.2.1 Complementation of naturally occurring His^- and Uro^- strains with histidine- and urocanate-specific transporter genes from *P. fluorescens* SBW25

To the test the hypothesis of transporter deficiency, I took advantage of the histidine- and urocanate-specific transporter genes (*hutTh* and *hutTu*) identified in *P. fluorescens* SBW25 and performed heterogeneous complementation in the His^+ Uro^- and His^- Uro^+ strains. In a previous work (Zhang, et al, 2012), *hutTh* and *hutTu* were cloned into the broad host range plasmid pME6010, resulting pME6010-*hutTh* and pME6010-*hutTu*. The two recombinant plasmids were introduced into 29 His^- and 25 Uro^- strains using a standard procedure of tri-parental plasmid conjugation (see Materials and Methods). The vector pME6010 was also conjugated into those strains as a negative control. The transconjugants were subjected to growth assay under the same conditions as described above, and the results were shown in detail in Table 3.4, and for the

isolates that restored growth, their growth differences compared to their wild type strains were shown more illustrately in Fig. 3.1. The original wild type isolates acting as additional controls were also included in the investigation and the results were the same as the pME6010 vector controls (Data not shown).

Table 3.4. Transporter complementation results of histidine and urocanate compromised isolates. OD450nm data were obtained by averaging three individual replicates. The isolates that successfully restored growth histidine or urocanate were marked with "*"

Isolates	Histidine OD450		Isolates	Urocanate OD450	
(His^-, Uro^+)	pME6010	pME6010-*hutTh*	(His^+, Uro^-)	pME6010	pME6010-*hutTu*
U118	0.31	0.68*	U165	0.32	0.30
U119	0.29	0.67*	U166	0.33	0.31
U121	0.20	0.60*	U212	0.14	0.59*
U128	0.12	0.14	U249	0.22	0.57*
U143	0.33	0.61*	U256	0.11	0.56*
U136	0.31	0.65*	U261	0.17	0.60*
U143	0.38	0.63*	X111a2	0.11	0.12
U148	0.35	0.65*	X111b1	0.14	0.11
U158	0.11	0.64*	X111b2	0.13	0.12
U159	0.10	0.63*	X113a1	0.13	0.15
U160	0.22	0.63*	X123a2	0.20	0.22
U161	0.21	0.61*	X143a1	0.23	0.21
U172	0.24	0.69*	X143a2	0.22	0.20
U173	0.20	0.68*	X151b1	0.25	0.51*
U176	0.17	0.60*			
U182	0.17	0.59*			
U184	0.18	0.60*			
U191	0.34	0.50*			
U194	0.22	0.59*			
U197	0.38	0.64*			
U203	0.19	0.61*			
U265	0.10	0.50*			

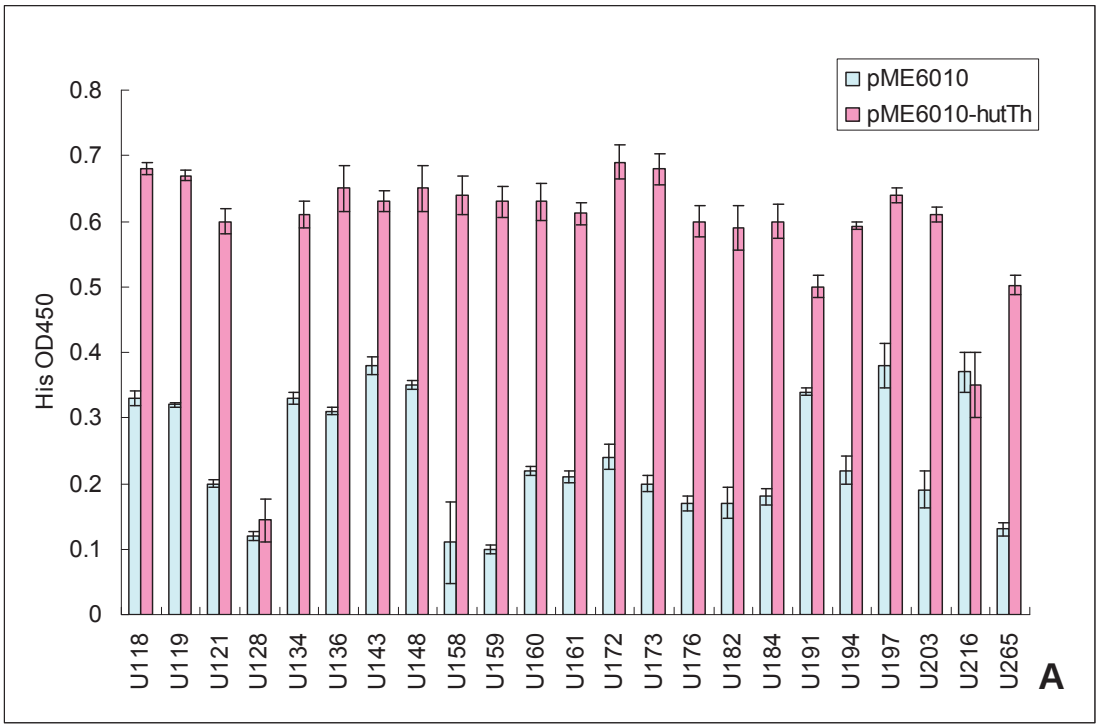

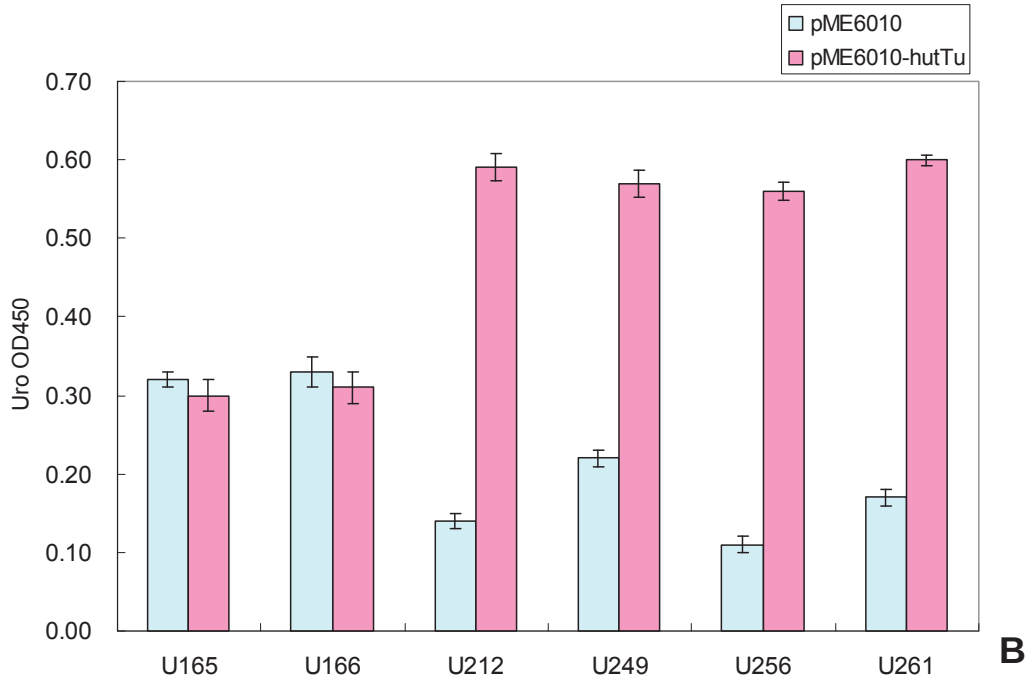

Fig. 3.1. Heterogeneous *hutTh* complementation of Oxford His$^-$ (A) and Uro$^-$ (B) strains. pME6010 vector complementation strains are shown as negative controls in blue and *hutTh* complementation strains in pink. Bars represent the mean, and the error bars represent 95% confidence intervals of the mean of 3 replicate individuals.

The introduction of functional urocanate transporters successfully restored 4 His$^+$, Uro$^-$ isolates to utilize urocanate as the sole carbon and nitrogen source.

In contrast, all the His^-, Uro^+ strains, with the only exception of U128, gained the ability to utilize histidine with the complementation of *hutTh*. Taken together, the obtained data clearly suggested the high level of histidine and urocanate metabolism variation in *Pseudomonas* with respect to the actual histidine and urocanate transport system in the *hut* genes.

3.2.2 Complementation of *hutH2* and genetic analysis of wild-type U128 *hutH2-hutTh* genes

The observed fact that the introduction of *hutTu* into U128 has minimal effect on its growth in histidine strongly suggested the functional histidase gene (*hutH2*) is either missing or not functional in its genome. To test this hypothesis, both *hutTh* and *hutH2* from *P.fluorescens* SBW25 were introduced into U128, along with the single U128-*hutH2* complementation as a control, the resulting dual recombinant isolate gained the ability to grow on histidine (Fig. 3.2). The fact that a single complementation of *hutTh* or *hutH2* was not sufficient to restore U128 to utilize histidine clearly indicating that isolate U128 lacks both a functional histidine transporter and a functional histidase in the genome.

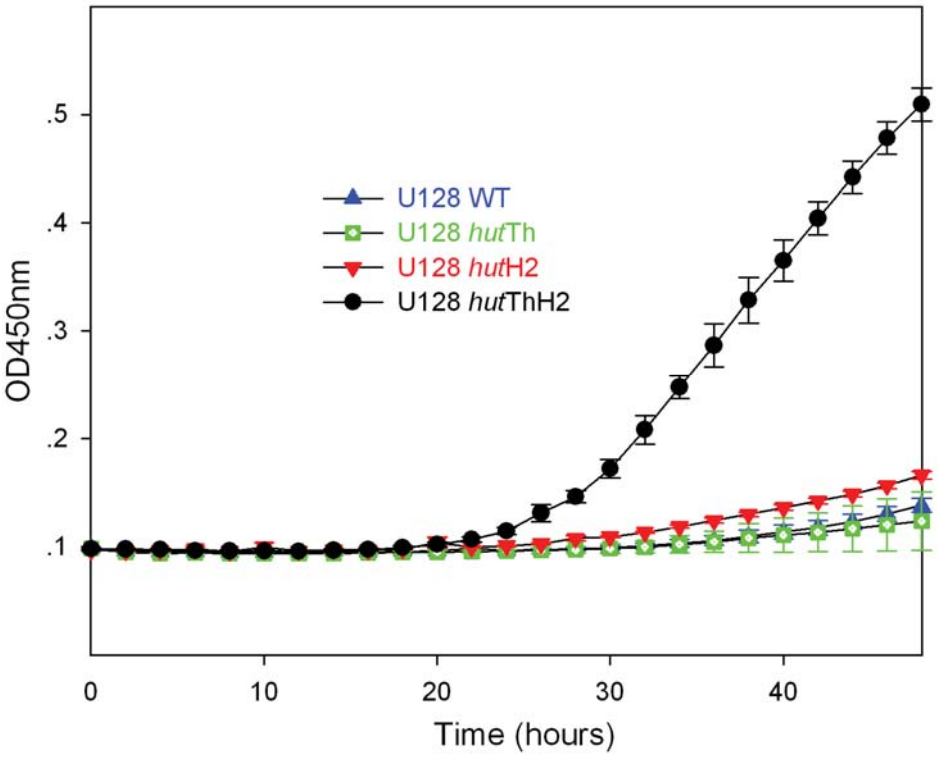

Fig. 3.2. Genetic complementations *hutTh* and *hutH2* in U128. The growth curves showing OD450 of wild-type (WT) U128, U128 complemented with *P. fluorescens* SBW25's histidine transporter, histidase and the both, respectively. Error bars represent standard errors. All values are the averages of three individuals.

Because the unique histidine utilization phenotypic characteristics of U128, investigations were done on the genetic basis of *hutH2* and *hutTh* from U128. Previous studies have determined the amino acid sequences of the histidase active sites, and they are highly conserved among *Pseudomonas* (Hernandez et al. 1993; Ro¨ther et al. 2001). A fragment of DNA sequence covering the active site from *hutH2* from U128 was successfully amplified by PCR and sequenced, however, no amino acid mutations were found in the active site of *hutH2* (See Fig. S1).

As *hutTh* is located between *hutH2* and *hutI* (Fig. 1.2), an approximately 2kb PCR fragment was successfully amplified from the U128 genome using a pair of designed universal primers H2F1 and IR (see Materials and Methods). Interestingly, the sequencing and alignment result clearly illustrated the presence of *hutH2* and *hut*I in U128, with no *hutTh* sequences detected between the two genes. *hutTh* is located in between *hutH2* and *hutI* in all the

His^+ sequenced *Pseudomonas (*Consevage et al. 1985; Hu et al. 1989; Allison and Phillips 1990; Stover et al. 2000; Joardar et al. 2005; Silby et al. 2009; Zhang et al. 2011), the finding was significant to suggest the lost of the expected histidine transporter between *hutH2* and *hutI* in U128. To our knowledge, this is the first time the data is able to show this deletion in *Pseudomonas.*

3.2.3 Investigation on Auckland His^- and Uro^- strains

A large portion (37%) of Auckland strains fall into the unique His^-, Uro^- phenotypic category, which is not found elsewhere (Table 3.1). Because of their unique phenotypes, whether or not the *hut* locus is present is still questionable. Investigations were done by applying PCR with universal hut primers hutH2F1 and hutH2R1 specific to *hutH2* region, attempting to screen for the evidences of *hut* operon's existence. Although 8/26 strains gave a PCR product, none of them were confirmed by subsequent sequencing to be *hutH2* (Dta not shown).

3.3 Multilocus sequence analysis (MLSA) of plant-associated *Pseudomonas*

The MLSA technique involves the following four steps: 1) preparation of bacterial genomic DNA, 2) PCR-amplification of the target genes, 3) DNA sequencing of the PCR products, and 4) phylogenetic analysis based on the obtained DNA sequences. A total of 230 phyllosphere-colonizing *Pseudomonas* strains were subjected to MLSA analysis (164 from Oxford, 66 from Auckland).

The initial analysis was performed by Drs. Robert Jackson and Dawn Arnold, aiming to analyze 7 house-keeping genes: *gapA* (glyceraldehyde 3-phosphate dehydrogenase), *gltA* (citrate synthase), *acnB* (aconitate hydratase), *gyrB* (gyrase B), *coxC* (cytochrome c oxidase), *pgi* (glucose- 6-phosphate isomerase), and *rpoD* (RNA polymerase sigma factor D). For each gene, two pairs of primers were designed to amplify the gene fragment, aiming to get approximately 400 nt, and subsequent DNA sequencing. All the primers are

listed in Table 2.3. However, the initial MLSA analysis was hampered by the difficulties of PCR amplification with many strains; only 6 strains (U130, U131, U132, U133, U1135, U185 and U196) resulted in successful sequencing of all the 7 genes.

The primary results suggested that the plant-associated *Pseudomonas* were genetically diverse and a MLSA analysis of 3-4 genes might be sufficient for estimating their genetic relatedness. Therefore, in this work I focused on the MLSA analysis of three house-keeping genes (*gapA*, *gltA* and *acnB*). Six pairs of primers were designed and listed in Table 2.3. As shown in Fig. 3.3, the three genes are almost equally distributed in the genome of *P. fluorescens* SBW25, and the similar genomic locations were found in other *Pseudomonas* strains whose genome sequences are currently available (See Fig. S2).

The DNA sequences of three genes were successfully obtained for a total of 155 strains (99 from Oxford and 56 from Auckland). As expected, all three genes display a higher polymorphism at the DNA level than at the amino acid level (Fig. 3.4). Importantly, all three genes contribute almost equally to the polymorphism of the *Pseudomonas* populations, which are analyzed based on concatenated sequences of three genes (Fig. 3.4).

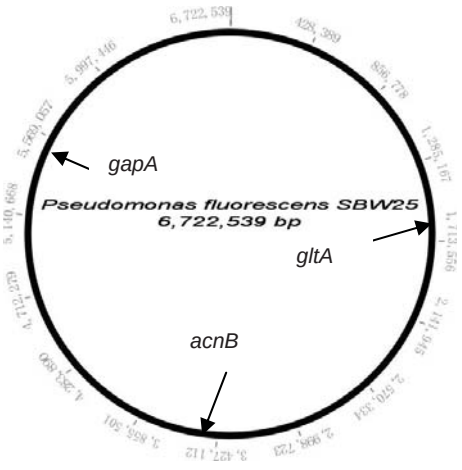

Fig. 3.3. Genomic locations of the three house-keeping genes in *P. fluorescens* SBW25. Each individual gene is indicated within the circular genome with the actual sizes of the genomes. Only *P.fluorescens* SBW25 genome is shown as other sequenced *Pseudomonas* genomes are showing similar patterns.

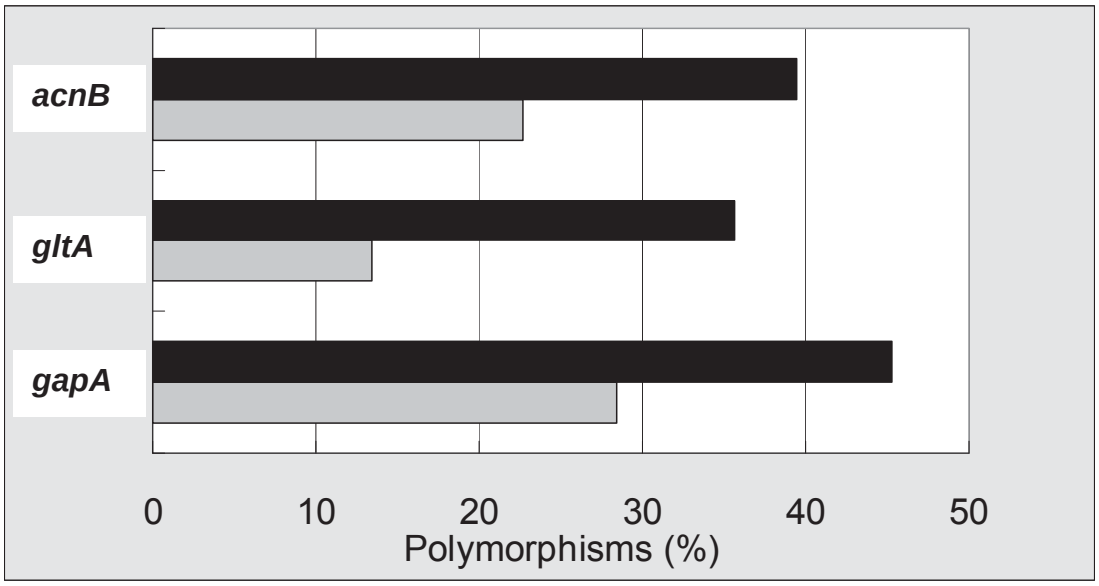

Fig. 3.4. Polymorphism levels for each house-keeping gene in *Pseudomonas*. Black bars reflect nucleotide polymorphisms and grey bars indicate amino-acid polymorphisms.

For each strain, the DNA sequences of three genes (615 nt for *gltA*, 303 nt for *gapA*, 273 nt for *acnB*) were concatenated and subjected to subsequent phylogenetical analysis. Representative Neighbor-Joining (NJ) trees are shown in Fig. 3.5 and Fig. 3.6. Data presented in Fig. 3.5 clearly showed that the *Pseudomonas* strains belong to two distinct groups, which are dominated by strains from Oxford (left cluster) and Auckland (right cluster), respectively. The four different phenotypes were shown by different colours (red for His^+ Uro^+; green for His^+, Uro^-, yellow for His^-, Uro^-, and blue for His^-, Uro^-). While His^+ Uro^+ strains are found both in Oxford and Auckland populations, His^- Uro^- strains are restricted to Auckland population.

Strains from Oxford and Auckland were analyzed separately and the resulted two NJ tress are shown in Fig. 3.6. Also shown is the phenotype of each strain in term of its ability to grow on histidine and urocanate. The results revealed a clear correlation between phenotypes and genotypes (Fig. 3.6). Strains with the same His and/or Uro phenotypes were mostly clustered in one group, with the exception strain 134 from Oxford (His^-, Uro^+, His OD450=0.37, sitting at the boarder of His^- and His^+ region) (Fig. 3.6 A). For Auckland population, there was a distinct boundary in between X151b1 and X123a1, which separated the His^+,

Uro$^+$ phenotype from other types (Fig. 3.6 B). Consistent with Oxford population, the same phenotypic strains are mostly grouped together.

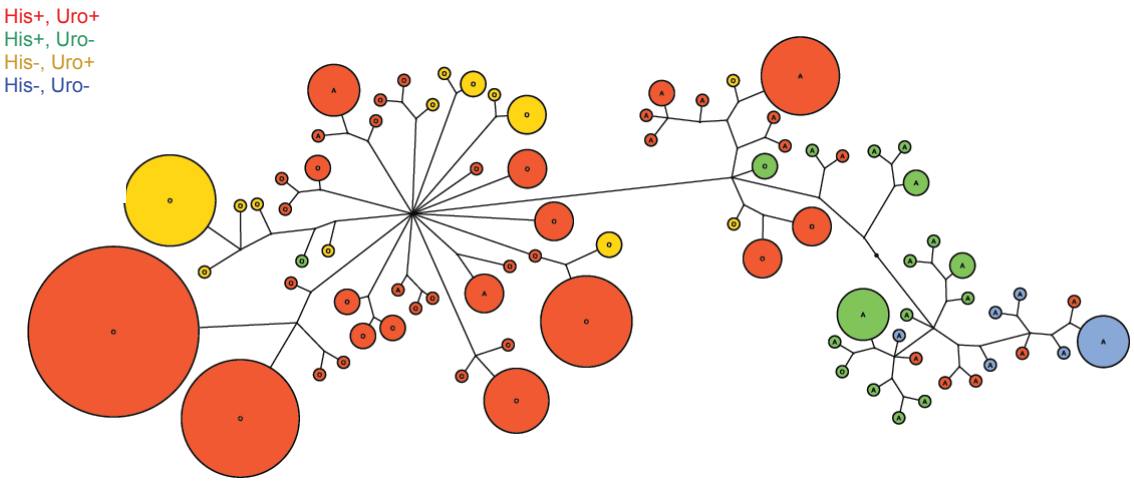

Fig.3.5. Unrooted phylogenetic tree showing the genetic relatedness between the Oxford and Auckland *Pseudomonas*. Distance calculations were using the NJ method with Kimura 2 correction. Letter "O" and "A" represented Oxford and Auckland respectively. The sizes of the grapes were proportional to the number of isolates and coloured according to the 4 His/Uro phenotypes showing in the figure.

Due to the sampling and naming principles that applied, the isolation location of each strain in this study could be tracked back to its origin of isolation in the sugar beet plant (See Materials and Methods). NJ trees were also constructed based on the individual sugar beet plant (Fig. S3). Strains with the same phenotypes still clustered together. Here, it is not surprising to see one leaf contribute to the identical phenotypes, as the strains were likely to be the same clones from the same ancestor which landed on one part of the leave and subsequently spread out through the entire leave surface.

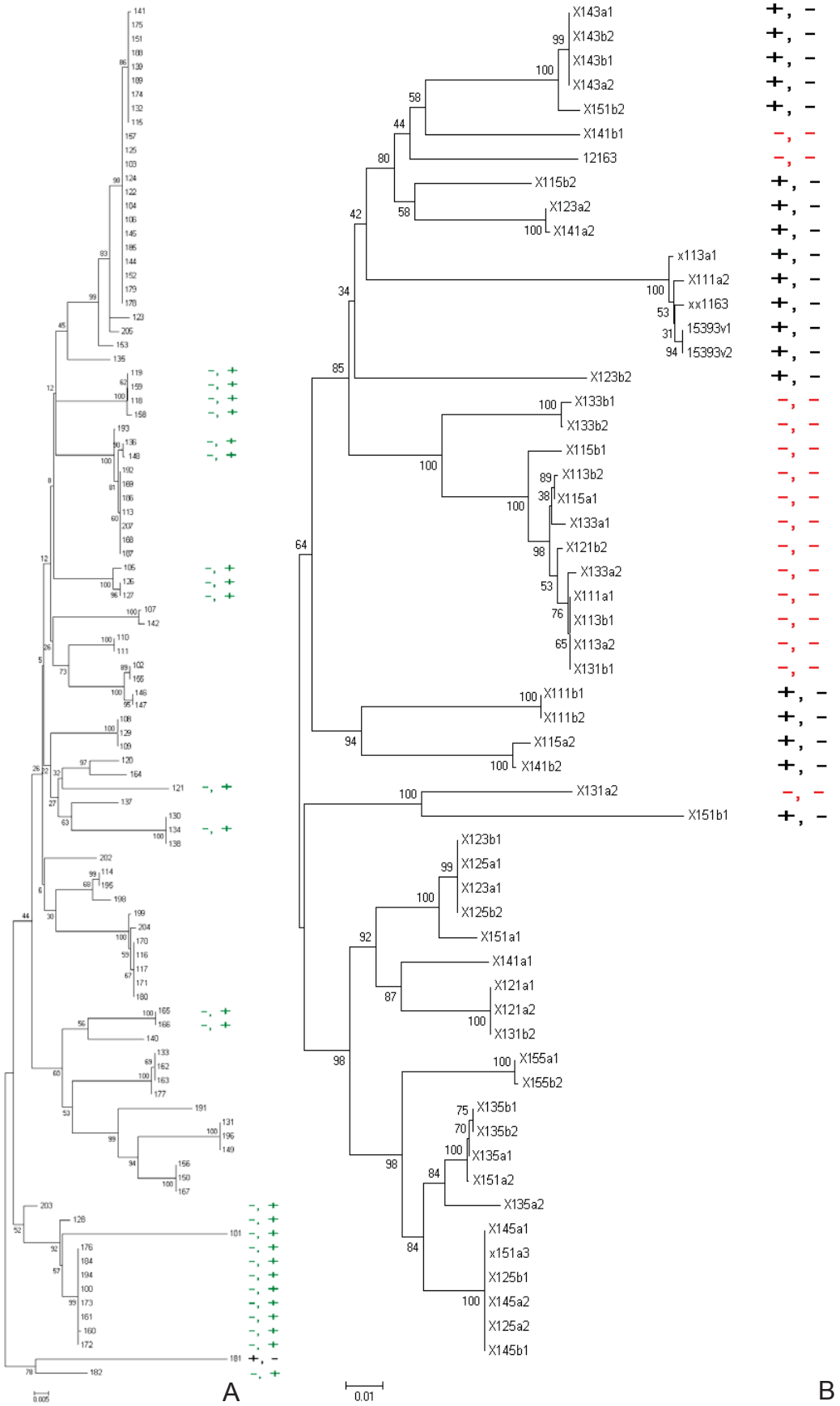

Fig. 3.6. Unrooted trees of the (A) Oxford population and (B) Auckland population. Tree were constructed with the obtained concatenated nucleotide sequences of 3

house-keeping genes (*gapA, gltA, and acnB*) using the NJ method with Kimura 2 correction for distance calculations. The total length of the concatenated group of nucleotide sequences was same as previous described. Bootstrap percentages retrieved in 1,000 replications are shown at the nodes. The scale bar indicates the number of nucleotide substitutions per site. The His/Uro phenotypes are coloured according to the following categories: +, - black, -, + green, and -, - red. The unlabelled strains represent His^+,Uro^+ phenotypes.

Chapter 4: Discussion

For any living organism, especially plant-colonizing bacteria, obtaining an adequate supply of critical nutrients is a key for survival. Carbon makes up the carbon-backbone of the majority of cellular molecules, and its availability in the environment, especially in soils, is limited. Under this natural selection force, many plant-associated bacteria have evolved mechanisms to cope with this carbon-limited environment. Taking up extracellular amino acids such as histidine for degradation is one example. Histidine contains both carbon and nitrogen in a ratio of 2:1, and has a putative role of being an important source of carbon, nitrogen, and energy. Additionally, histidine can be directly used for bacterial DNA translation.

The ecological success of *Pseudomonas* in plant environments is largely determined by the phenotypes that it expresses: these can allow efficient utilization of nutrients derived from hosts which is fundamentally important for bacterial competitiveness on plant surfaces (Rainey et al. 1994; Thompson et al. 1995; Rainey 1999; Nishijyo et al. 2001; Rico and Preston 2008; Zhang and Rainey 2008). Unsurprisingly then, *Pseudomonas* up-regulates the expression of many genes involved in nutrient scavenging. An example is the *hut* genes dedicated to the uptake and degradation of histidine and urocanate (Rainey 1999; Zhang and Rainey 2007). This locus was also up-regulated under low temperature conditions (Kannan et al. 1998).

Previous research has shown that many *Pseudomonas* including *P. fluorescens* SBW25 have a gene encoding for a histidine-specific transporter so that the bacteria are capable utilizing histidine as the sole carbon and nitrogen source (Hu and Phillips 1988; Zhang and Rainey 2007). *E.coli* cannot utilize histidine directly due to its lack of degradative enzymes, which suggests that one of the reasons for the ecological success of *Pseudomonas* species in the natural environment is their ability to utilize histidine.

Phenotypic variation is predominantly determined by natural selection. Even though phenotypic variation is abundant and easy to observe, the genetic basis is less understood (Barton and Turelli 1989; Flint and Mott 2001). In this study, the ability to utilize histidine and urocanate was tested in 230 natural *Pseudomonas* isolates, which revealed interesting polymorphism. Histidine utilization in *Pseudomonas* has been previously investigated in model organisms of *P. putida* (George and Phillips 1970; Itoh et al. 2007), *P. fluorescens* SBW25 and *P. aeruginosa*, however, this study extends this to a natural population level.

The *Pseudomonas* populations in this study exibited four His and Uro phenotypes: His^+, Uro^+; His^+, Uro^-; His^-, Uro^+; and His^-, Uro^- (Table 3.1). In the histidine- or urocanate-impaired strains, His^-, Uro^+ were more prevalent in the Oxford population studied, whereas for the Auckland population the opposite was found with His^+, Uro^- dominant. Additionally, the His^-, Uro^- phenotype was found to be present only in the Auckland population. These results strongly suggest that during evolution, like other non-house keeping genes, the major *hut* metabolic genes are highly conserved among *Pseudomonas* but the transporter genes are not. This is supported by the majority of the wild *Pseudomonas* isolates in this study being capable of utilizing histidine and/or urocanate as the sole carbon and nitrogen source. In order to do so, all the major *hut* metabolite genes must be present and functional (Fig. 1.1 and Fig. 1.2) (Hu and Phillips 1988; Zhang and Rainey 2007). Therefore, the presence of the four phenotypes, especially His^+, Uro^- led to the hypothesis that the phenotypic variation was due to lack of functional histidine and/or urocanate transporters in the His^- and Uro^- isolates.

Therefore a heterogeneous complementation study was undertaken in the His^- and Uro^- *Pseudomonas,* proving the above hypothesis to be correct (Fig. 3.1). The introduction of *P. fluorescens* SBW25 histidine or urocanate transporters restored the ability of the majority of the naturally histidine-impaired and approximately $1/3^{rd}$ of the urocanate-impaired Oxford *Pseudomonas* to grow on histidine or urocanate, respectively (Table 3.4 and Fig. 3.1). However, isolate U128 (naturally His^-, Uro^+) did not become His^+ until both copies of the histidine transporter and a functional histidase were introduced into its genome (Fig. 3.2).

Further genetic analysis revealed that U128 has lost its histidine transporter gene during evolution (Fig. 3.3). This provided further evidence to support the hypothesis that phenotypic variation is due to the presence of absence of histidine and urocanate transport systems from the *hut* genes, not presence of absence of major metabolic genes, to be true.

Many evolutionary analyses of gene malfunctions have been attributed to the "use it or lose it" principle: in order to cope with constant fluctuations in the environment, some infrequently used and non-essential gene components are selectively deleted from the host's genome, and with those deletion mutations, the hosts are able to adapt to new ecological niches with a higher fitness (Stover et al. 2000; Liman 2006). The *hut* genes are metabolite-non-essential genes for *Pseudomonas,* but their presence enables the host to utilize histidine as the sole carbon and nitrogen source, which is likely to improve ecological performance in the natural environment (Zhang et al. 2006; Zhang and Rainey 2008). The data from the present study suggests that U128 is exposed to urocanate in its environmental niche and has become a urocanate utilization expert, so eventually the genes encoding for histidine transporter and functional histidase became redundant and subsequently lost during the evolutionary process.

There are two theories that explain genetic tradeoffs in evolution (the term "tradeoff" in this study refers to the presence of four His/Uro phenotypes in the population rather than only one phenotype): antagonistic pleiotropy and mutation accumulation (Williams 1957; Lynch and Gabriel 1987; Wilson and Yoshimura 1994; MacLean et al. 2004). The first theory applies when mutation occurs on a single gene, which encodes multiple traits, and such mutation will enhance an individual's fitness in one environment but will have a negative impact on fitness in the other environment. The latter one describes a situation where a gene is not in use so that mutations accumulate and eventually cause malfunction or deletion of that gene and cause phenotypic change. In this research, the results obtained from the complementation study fit the theory of mutation accumulation, as mutations in histidine/urocanate transporter genes alone have neutral effects on the rest of the *hut* genes as they are not

housekeeping genes. Additionally, antagonistic pleiotropy does not appear to be general for transporter gene mutations. In conclusion, based on the obtained data in this study, mutation accumulation is more likely to be the driving force to explain the phenotypic variations (tradeoffs) of the *Pseudomonas* populations that were examined. This hypothesis could be further tested by examining the nutrient composition (including amino acids, vitamins and minerals) on the sugar beet leaf surfaces by extraction and HPLC, LCMS/MS, or ICP-MS.

Another finding in this study was the identification of 29 His^-, Uro^+ *Pseudomonas* isolates in the Oxford population (Table 3.1). Urocanate is excreted through human sweat glands and is commonly found in human stratum corneum due to the absence of urocanase in the skin (George and Phillips 1970; Kessler et al. 2004). Many epidermal microflora are able to utilize urocanate as the sole carbon and nitrogen source (Hug et al. 1999). However, *Pseudomonas* are not commonly found on the human stratum corneum except for *P. aeruginosa* which is commonly found in the lungs of patients with cystic fibrosis, so the presence of Uro^+ plant-associated *Pseudomonas* isolates in this study is unexplained.

One explanation could be the presence of urocanate in the environment (sugar beet leaves). Urocanate absorbs UV light so urocanate in stratum corneum acts as a natural endogenous sunscreen or photoprotectant against UV radiation causing DNA damage (Kavanagh et al. 1995; Kammeyer et al. 1997; Hug et al. 1999; Norval et al. 2008). The identification of Uro^+ *Pseudomonas* suggests the presence of urocanate in the environment, and possibly the sugar beet leaf surfaces, acting as a photoprotectant. Along with testing the hypothesis of mutation accumulation discussed above, use of HPLC or LCMS/MS to analyse for the presence of urocanate on the sugar beet plant surfaces could be worthy of future research.

Understanding the population structure and the phylogenetic relationships among *Pseudomonas* strains in the natural environment is essential in order to explain their ecological success. In theory, the biogeographical presence and distribution of bacteria can be interpreted either by environmental variations or historical events (Khan et al. 2008). The former idea predominantly describes

the effects of natural selection, which is the natural forces acting on individuals and selecting the individuals with the best fitness. For example, the presence of Uro^+ strains in the present study were most likely selected by natural selection on sugar beet leaf surfaces due to the presence of urocanate accumulated in the environment, as discussed above. The latter idea is more abstract, and it describes a random event that alters either the population structure in the community, or the genetic flow between individuals. The example here would be the spreading/distrubuting of bacteria by animals moving within their home range. In this study, the positive correlation of phylogenetic and genotypic characteristics suggests that environmental variations may have contributed to the two distinct population structures observed in this study. The effects of such variations acting on the *Pseudomonas* population on sugar beet leaf surfaces may be at an early stage of natural selection. Evidence for this is that only U128 was found to have dual mutations in *hutH2* and *hutTh* in this study. With continued evolution, the His^-, Uro^+ *Pseudomonas* isolates may become more urocanate-utilizing specialsts and eventually lose *hutH2,* according to the "use it or lose it" principle discussed above.

The MLSA technique provides a powerful tool to understand the genetic relationships of populations simply by sequencing a short PCR product (Maiden et al. 1998; Tavanti et al. 2005). It has been applied in many population genetic studies previously, and these include both pathogenic and non-pathogenic bacteria (Chan et al. 2001; Adiri et al. 2003; Pérez-Losada et al. 2006; Khan et al. 2008). In the final part of this study, MLSA was utilized to investigate the correlations between phenotypes and genotypes as well as how the populations were genetically related. By choosing three house-keeping genes as the dataset, the NJ trees clearly revealed the close relationship between phenotypes and genotypes (Fig. 3.5 and Fig. 3.6). In most cases, only the same His/Uro strains were genetically clustered together, a significant finding of this study.

Unlike other population genetic studies which have used environmental isolates directly from a pond, lake or general environment, the *Pseudomonas* isolates used in this study came from two clearly labelled and specifically described sugar beet fields (Oxford, UK and Auckland, New Zealand), making the exact

source of each strain traceable (Fig. S3). Correlating the origin of isolates with the phenotypic characteristics, showed that the same phenotype was exclusively gathered in one cluster and there was no mixture of different phenotypes in a cluster. Predominantly, one sugar beet leaf contributed to one phenotype (two isolates from each leaf). This was particular so in the Auckland isolates (see Fig. S3), although it is possible that both isolates from the same leaf were replicates and genetically identical.

The phylogenetic tree constructed based on the MLSA sequence showed a clear separation of the two geographic populations, with some low degree of cross-over between them (Fig. 3.5). By applying the same strain isolation procedure, the only difference between the two populations was due to geographical location (Oxford vs Auckland). This suggests that the geographical factor may be the major factor explaining the two distinct populations. Overall, the MLSA data presented here indicates that it can be used as a powerful tool for studying population evolution, epidemiology, and genetics.

Appendices

Appendix A: Supplementary figures

```
SBW25_H2          SLSRGFSGIRRQVIDALIALINAEVYPHIPLKGSVGASGDLAPLAHMSLVLLGEGKARYK 166
PFL_0407          SLSRGFSGIRRQVIDALIALINAEVYPHIPLKGSVGASGDLAPLAHMSLVLLGEGKARYK 168
U128_h2           SLSRGFSGIRRQVIDALIALINAEVYPHIPLKGSVGASGDLAPLAHMSLVLLGEGKARYK 149
NT02PF0376        SLSRGFSGIRRVVIDALIALINAEVYPHIPLKGSVGASGDLAPLAHMSLVLLGEGKARHK 166
Psyr_4833         SLSRGSSGIRRVVIDALIALINAEVYPHIPLKGSVGASGDLAPLAHMSLVLLGEGKARYK 171
PSPPH_4865        SLSRGFSGIRRVMIDALIALINAEVYPHIPLKGSVGASGDLAPLAHMSLVLLGEGKARYK 171
PSPTO_5275        SLSRGFSGIRRVVIDALIALINAEVYPHIPLKGSVGASGDLAPLAHMSLVLLGEGKARHK 171
PP5032            SLSRGFSGIRRKVIDALIALVNAEVYPHIPLKGSVGASGDLAPLAHMSLVLLGEGKARYK 166
Pput_4906         SLSRGFSGIRRKVIDALIALVNAEVYPHIPLKGSVGASGDLAPLAHMSLVLLGEGKARYK 166
PSEEN5096         SLSRGFSGIRRKVIDALIALVNAEVYPHIPLKGSVGASGDLAPLAHMSLVLLGEGKARYK 166
PAO1_PA5098       SLARGFSGIRRKVIDALIALINAEVYPHIPLKGSVGASGDLAPLAHMSLVLIGESRARHR 165
PA14_67320        SLARGFSGIRRKVIDALIALINAEVYPHIPLKGSVGASGDLAPLAHMSLVLIGESRARHR 165
PSPA7_5831        SLARGFSGIRRKVIDALIALLNAEVYPHIPLKGSVGASGDLAPLAHMSLLLIGESKARHR 180
                  **:** ***** :*******:***************************:*:**.:**::
```

Fig. S1. *hutH2* sequence alignment of all the sequenced *Pseudomonas* including U128. The sequences are high conserved among individuals and the histidase active site of all the strains are circled with black box. The order of the strains are as follow: *P. fluorescens* SBW25, *P. fluorescens* PF1, U128, *P. fluorescens* PF5, *P. syringae* B728a, *P. syringae* 1448A, *P. syringae* DC3000, *P. putida* KT2440, *P. putida* F1, *P. entomophila* L48, *P. aeruginosa* PAO1, *P. aeruginosa* PA14, and *P. aeruginosa* PA7.

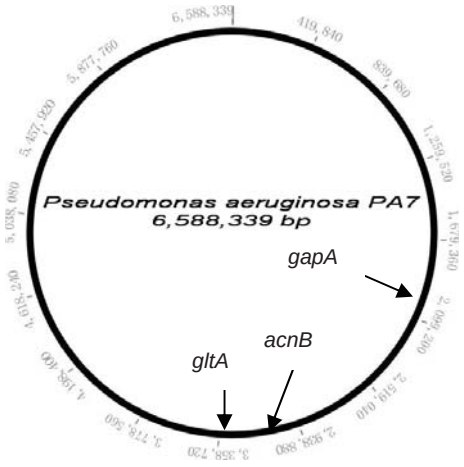

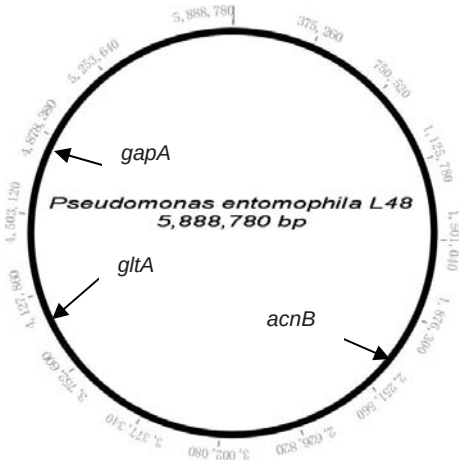

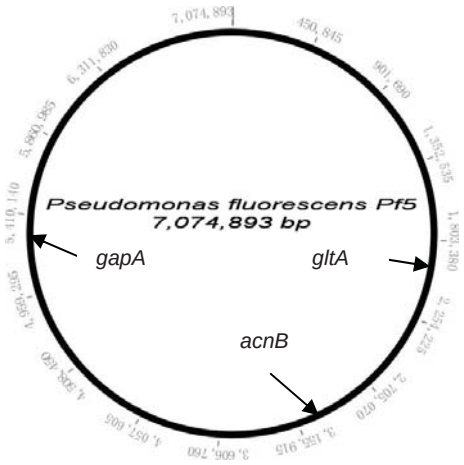
Pseudomonas fluorescens Pf5
7,074,893 bp
gapA
gltA
acnB

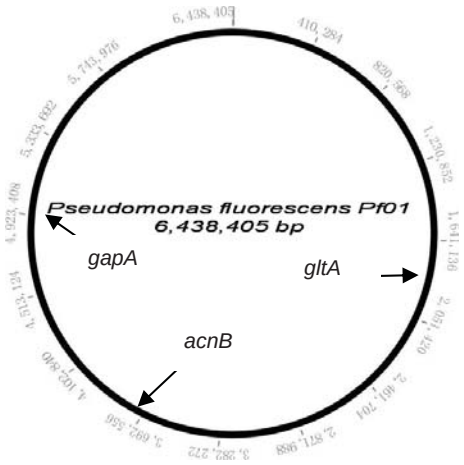
Pseudomonas fluorescens Pf01
6,438,405 bp
gapA
gltA
acnB

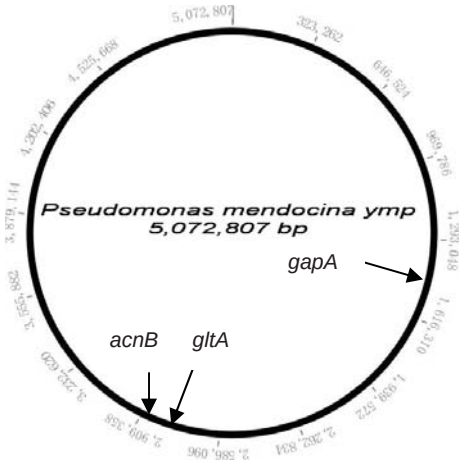
Pseudomonas mendocina ymp
5,072,807 bp
gapA
acnB
gltA

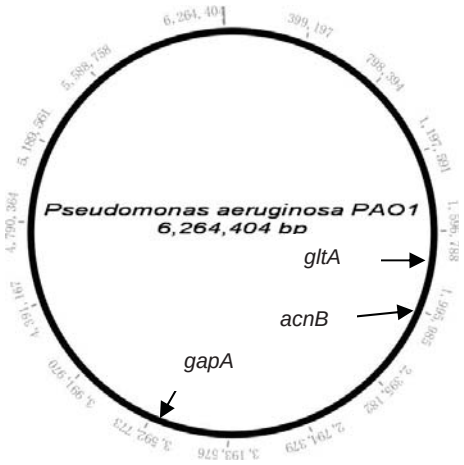
Pseudomonas aeruginosa PAO1
6,264,404 bp
gltA
acnB
gapA

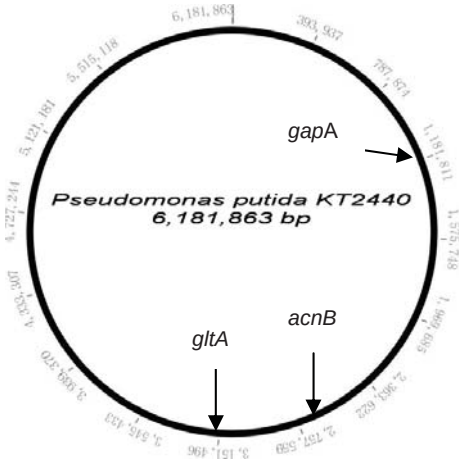
Pseudomonas putida KT2440
6,181,863 bp
gapA
gltA
acnB

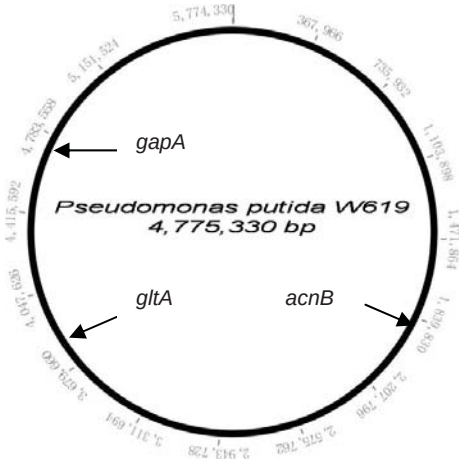
Pseudomonas putida W619
4,775,330 bp
gapA
gltA
acnB

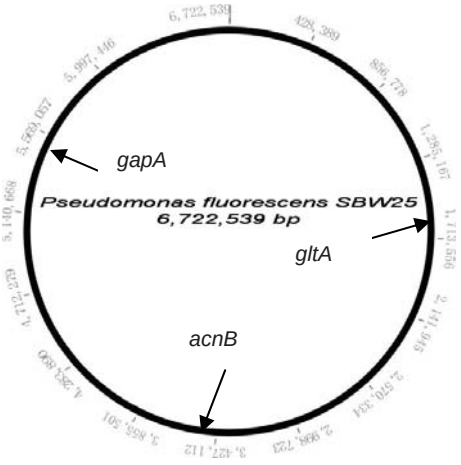

Fig. S2. Genomic locations of the three house-keeping genes in genome sequence available *Pseudomonas*. Each individual species is indicated within the circular genome with the actual sizes of the genomes. The arrows indicated the actual gene locations of the 3 selected house-keeping genes.

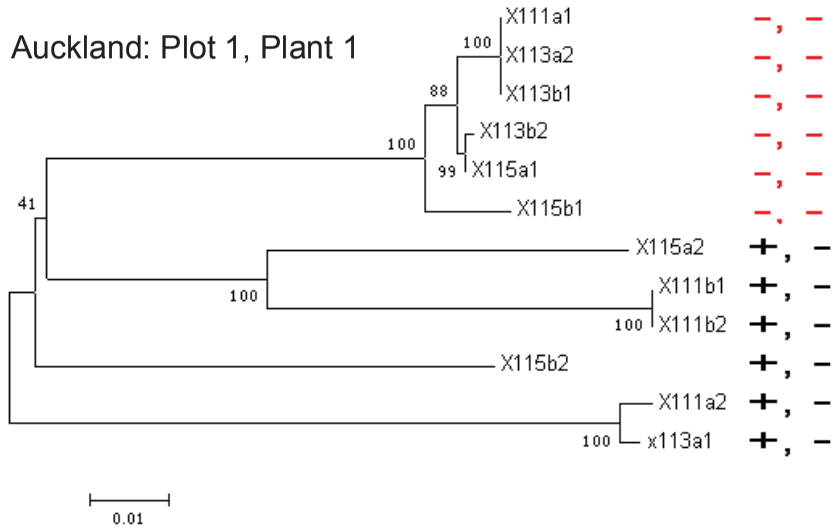
Auckland: Plot 1, Plant 1
X111a1
X113a2
X113b1
X113b2
X115a1
X115b1
X115a2
X111b1
X111b2
X115b2
X111a2
x113a1
100
88
100
99
41
100
100
100
0.01
−, −
−, −
−, −
−, −
−, −
−, −
+, −
+, −
+, −
+, −
+, −
+, −

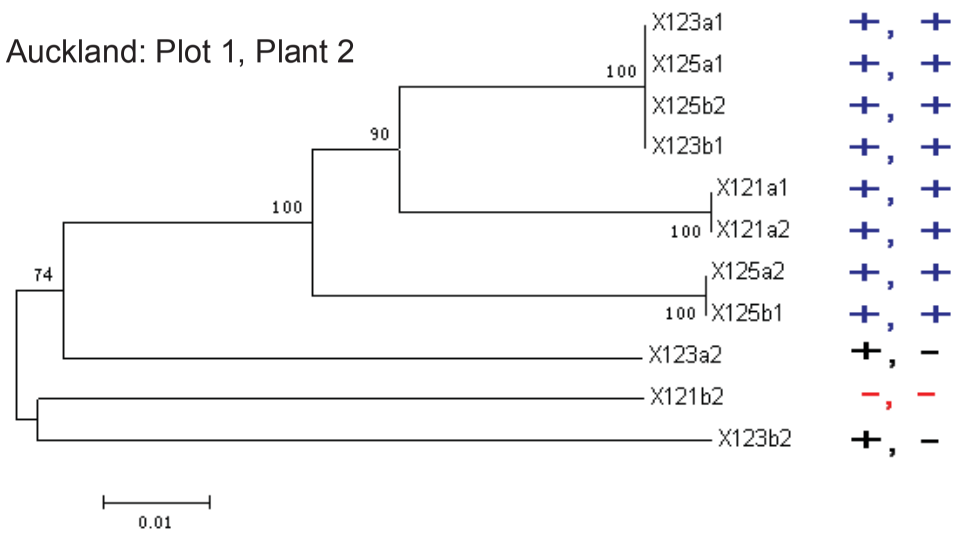
Auckland: Plot 1, Plant 2
X123a1
X125a1
X125b2
X123b1
X121a1
X121a2
X125a2
X125b1
X123a2
X121b2
X123b2
100
90
100
100
74
100
0.01
+, +
+, +
+, +
+, +
+, +
+, +
+, +
+, +
+, −
−, −
+, −

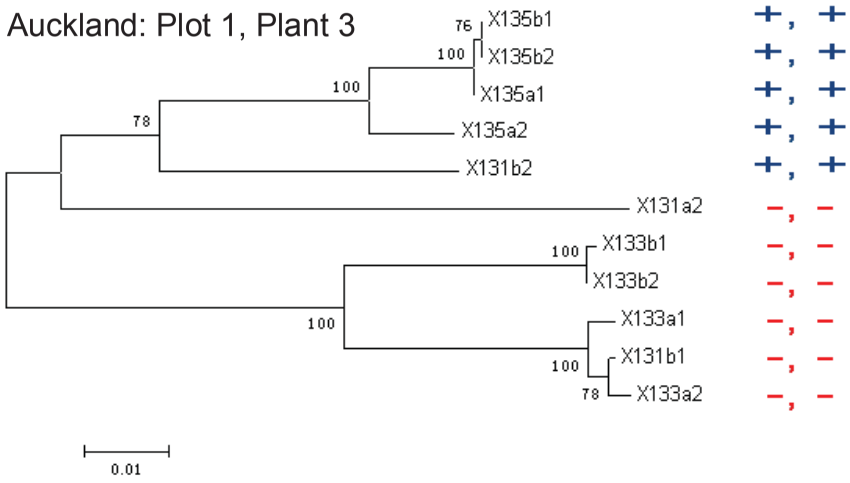
Auckland: Plot 1, Plant 3
X135b1
X135b2
X135a1
X135a2
X131b2
X131a2
X133b1
X133b2
X133a1
X131b1
X133a2
76
100
100
78
100
100
100
78
0.01
+, +
+, +
+, +
+, +
+, +
−, −
−, −
−, −
−, −
−, −
−, −

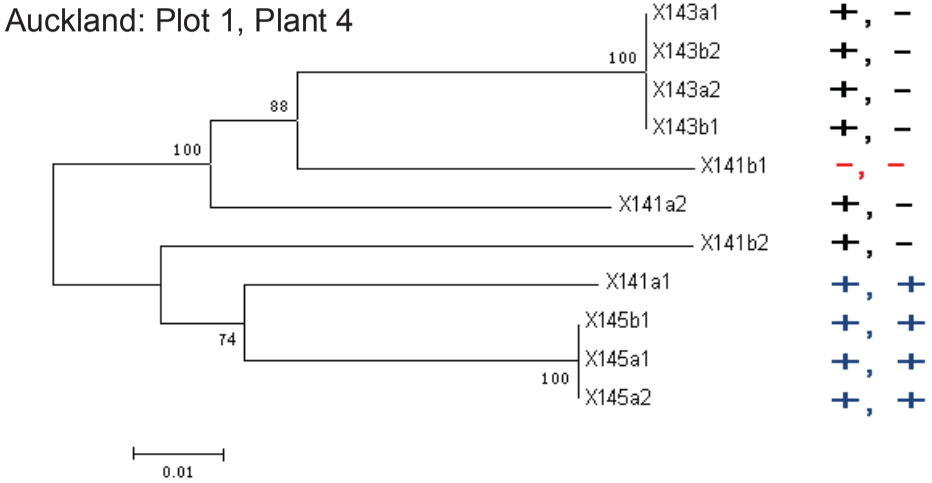
Auckland: Plot 1, Plant 4
X143a1
X143b2
X143a2
X143b1
X141b1
X141a2
X141b2
X141a1
X145b1
X145a1
X145a2
100
88
100
74
100
0.01
+, −
+, −
+, −
+, −
−, −
+, −
+, −
+, +
+, +
+, +
+, +

Auckland: Plot 1, Plot 5

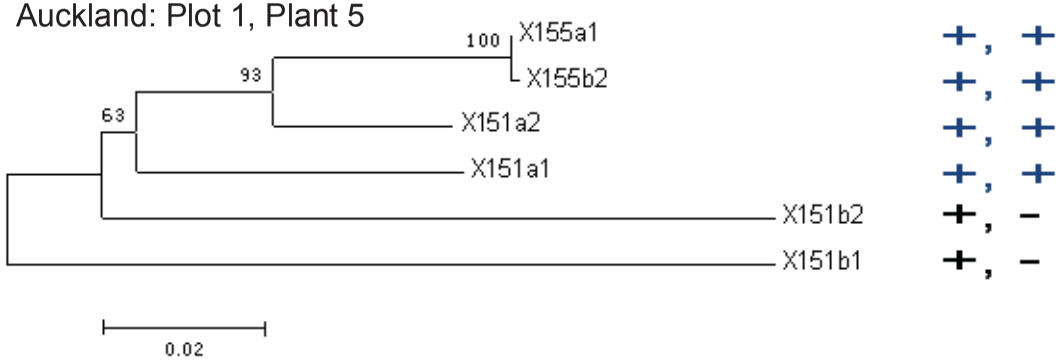

(B)

Oxford: Plot 3, Plot 1

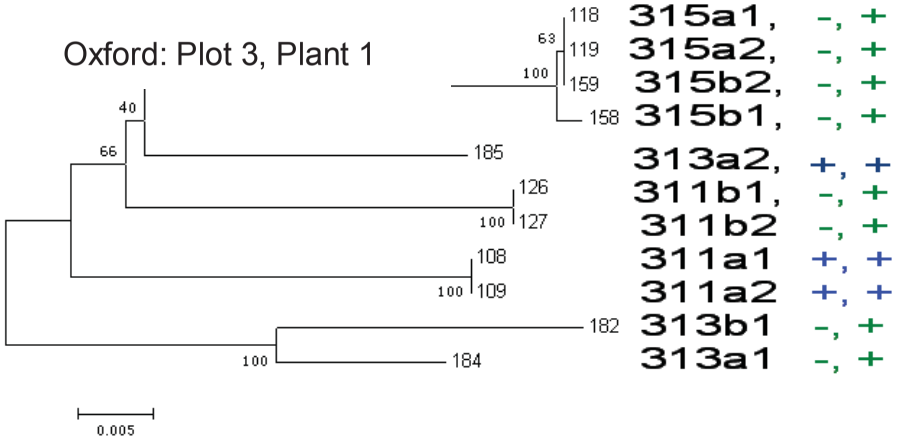

Oxford: Plot 3, Plant 2

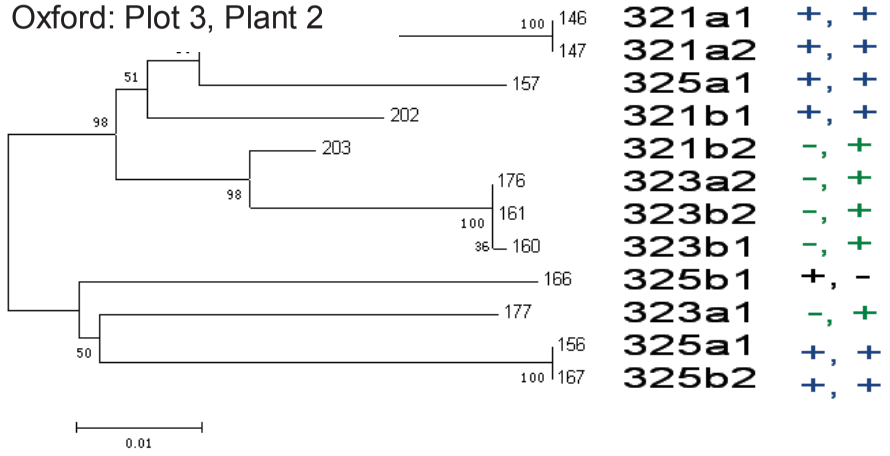

Oxford: Plot 3, Plot 3

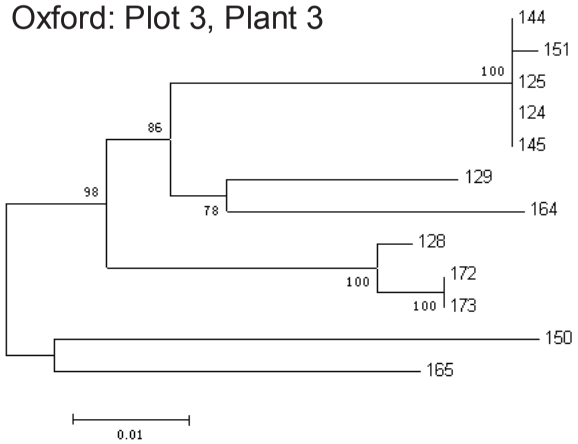

325b2	+,	+
333a2	+,	+
335a2	+,	+
335a1	+,	+
335b1	+,	+
331b2	+,	+
333b1	+,	+
331b1	−,	+
331a1	−,	+
331a2	−,	+
333a1	+,	+
333b2	+,	−

Oxford: Plot 4, Plot 1

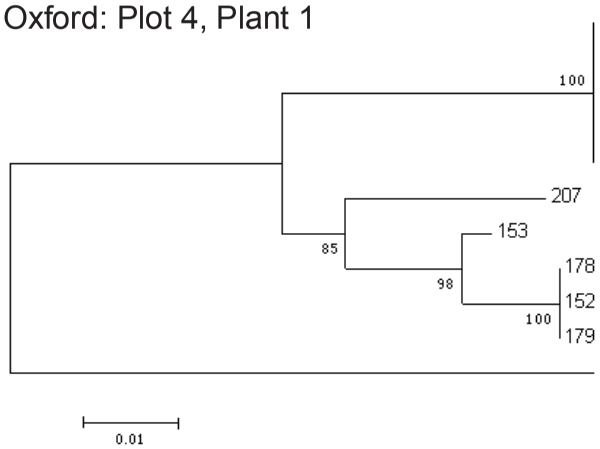

413a1	+,	+
413a2	+,	+
413b1	+,	+
411b1	+,	+
413b2	+,	+
411a2	+,	+
415b2	+,	+
415a1	+,	+
415b1	+,	+
415a2	+,	+
411b2	+,	−

Oxford: Plot 4, Plot 2

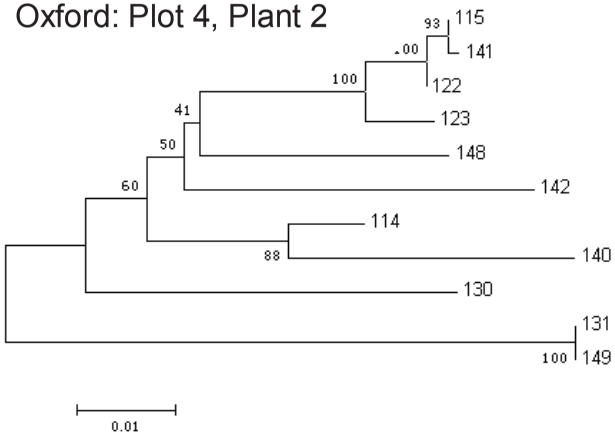

425a2	+,	+
425b2	+,	+
421b1	+,	+
421b2	+,	+
423b1	−,	+
421a1	+,	+
425a1	+,	+
425b1	+,	+
423a1	+,	+
423a2	+,	+
423b2	+,	+

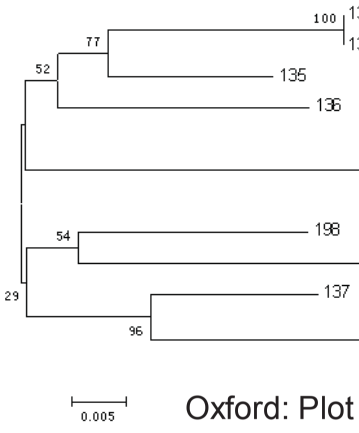

435a1	+,	+
431b2	+,	+
431a1	+,	+
433b1	−,	+
435a2	No data	
435b1	No data	
435b2	No data	
433a2	+,	+
433a1	+,	+
433b2	+,	+
431a2	−,	+
431b1	+,	+

Oxford: Plot 4, Plot 3

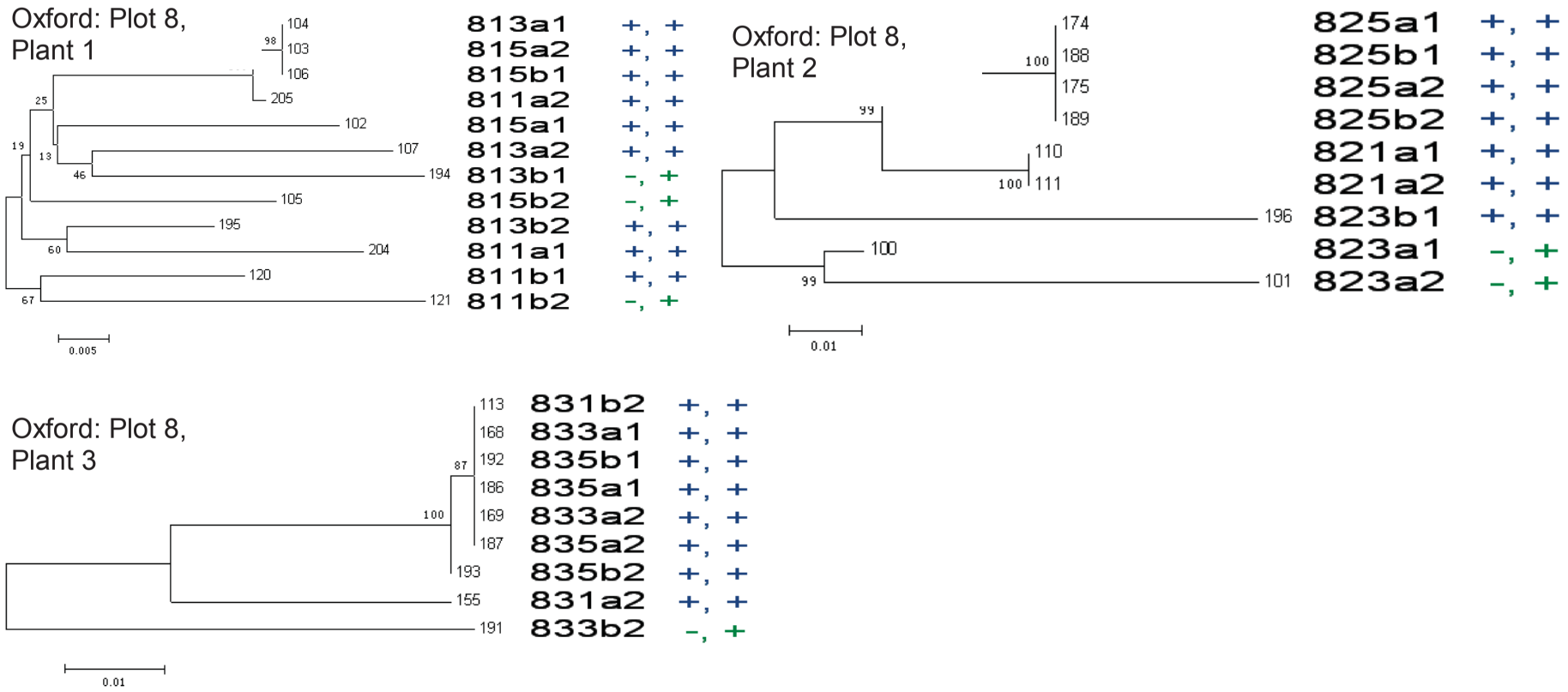

Fig. S3. Correlations between populations sampling origin locations and the His/Uro utilization phenotypes. The strains coding and origins refer to descriptions in Table 2.1, and the exact plot and plant numbers were indicated on each figure. The first plus symbol represents the His phenotype whereas the latter represents that of Uro. The trees were constructed using concatenated nucleotide sequences using the NJ method with Kimura 2 correction for distance calculations. Bootstrap percentages retrieved in 1,000 replications are shown at the nodes. The scale bar indicates the number of nucleotide substitutions per site. The His/Uro phenotypes are coloured according to the following categories: +, + blue, +, - black, -, + green, and -, - red.

Appendix B: Publication related to this study

Environmental Microbiology (2012) doi:10.1111/j.1462-2920.2011.02692.x

Variation in transport explains polymorphism of histidine and urocanate utilization in a natural *Pseudomonas* population

Xue-Xian Zhang,[1]* Hao Chang,[1] Sieu L. Tran,[2] Jonathan C. Gauntlett,[1] Gregory M. Cook[2] and Paul B. Rainey[1,3]

[1]*NZ Institute for Advanced Study, Massey University, Auckland 0745, New Zealand.*

[2]*Department of Microbiology and Immunology, University of Otago, Dunedin 9054, New Zealand.*

[3]*Max Planck Institute for Evolutionary Biology, Plön 24306, Germany.*

Summary

Phenotypic variation is a fundamental requirement for evolution by natural selection. While evidence of phenotypic variation in natural populations abounds, its genetic basis is rarely understood. Here we report variation in the ability of plant-colonizing *Pseudomonas* strains to utilize histidine, and its derivative, urocanate, as sole sources of carbon and nitrogen. From a population of 164 phyllosphere-colonizing *Pseudomonas* strains, 77% were able to utilize both histidine and urocanate (His^+, Uro^+) as growth substrates, whereas the remainder could utilize histidine, but not urocanate (His^+, Uro^-), or vice versa (His^-, Uro^+). An *in silico* analysis of the *hut* locus, which determines capacity to utilize both histidine and urocanate, from genome-sequenced *Pseudomonas* strains, showed significant variation in the number of putative transporters. To identify transporter genes specific for histidine and urocanate, we focused on a single genotype of *Pseudomonas fluorescens*, strain SBW25, which is capable of utilizing both substrates. Site-directed mutagenesis, combined with [^{3}H]histidine transport assays, shows that $hutT_u$ encodes a urocanate-specific transporter; $hutT_h$ encodes the major high-affinity histidine transporter; and *hutXWV* encodes an ABC-type transporter that plays a minor role in histidine uptake. Introduction of cloned copies of $hutT_h$ and $hutT_u$ from SBW25 into strains incapable of utilizing either histidine, or urocanate, complemented the defect, demonstrating a lack of functional transporters in these strains. Taken together our data show that variation in transport systems, and not in metabolic genes, explains a naturally occurring phenotypic polymorphism.

Received 18 October, 2011; revised 22 November, 2011; accepted 2 December, 2011. *For correspondence. E-mail x.x.zhang1@massey.ac.nz; Tel. (64) 9 414 0800; Fax (64) 9 414 8142.

Introduction

The ability to acquire nutrients is of fundamental importance for all organisms. Amino acids are especially valuable sources of carbon, nitrogen and energy for bacteria. Acquisition is typically a two-step process in which nutrients are first taken up from the environment via specialized transporters and then metabolized by substrate-specific enzymes. Given the availability of amino acids in many environments, particularly those involving a eukaryotic host (Simons *et al*., 1997; Phillips *et al*., 2004; Rediers *et al*., 2005), it would make sense for bacteria to have uptake and degradation systems for all 20 amino acids. However, this is rarely the case; of note is the fact that even closely related strains display variation in the profile of substrates utilized for growth. For example, from a set of 66 *Pseudomonas* isolates from milk, Wiedmann and colleagues (2000) showed that each strain possessed a unique pattern of substrate utilization. The causes of such variation, along with its molecular bases, are unknown. From a genetic perspective, the variation could stem from presence/absence polymorphisms in transporters, metabolic enzymes, or a combination of both.

In the plant growth-promoting bacterium *Pseudomonas fluorescens* SBW25, histidine is degraded by a five-step pathway with glutamate, formate and ammonia as the end-products (Zhang and Rainey, 2007a). Each of the five enzymatic reactions is catalysed by the gene products of *hutH, hutU, hutI, hutF* and *hutG*. As summarized in Fig. 1, the *hut* genes are organized in three transcriptional units (*hutF*, *hutCD* and *hutU-G*), with transcription being regulated by the HutC repressor (Zhang *et al*., 2006; Zhang and Rainey, 2007a). Activation of *hut* genes involves the interplay of two two-component regulatory systems (CbrAB and NtrBC) responsive to the availability of alternative carbon or nitrogen sources (Zhang and Rainey, 2008; Zhang *et al*., 2010). While preceding studies have

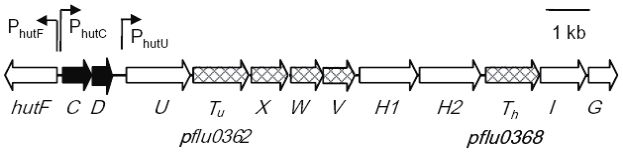

Fig. 1. Genetic organization of the *P. fluorescens* SBW25 *hut* locus. The metabolic *hut* genes and the *hut* regulators are shown by white and black arrows respectively. Crosshatched arrows represent genes encoding transporters described in this report. The *hut* genes are organised in three transcriptional units (operons) which expression is induced by histidine or urocanate (Zhang and Rainey, 2007a). Location of the promoters is indicated by vertical arrow-lines.

focused on *hut* catabolism and regulation, transporter genes responsible for the uptake of histidine and urocan- ate from external environments have not been elucidated.

Histidine transport in bacteria is complex and involves multiple systems with varying specificity and affinity. In the best-studied organism, *Salmonella typhimurium*, histidine is transported by at least five systems (Ames *et al*., 1977; Ames, 1985). The most specific system is a high-affinity permease designated HisJQMP, with HisJ a periplasmic binding protein (K_m, ~ 0.01 μM), two integral membrane proteins HisQ and HisM, and a single type of ATPase subunit (HisP), which exists as a homodimer in the membrane-bound complex $HisQMP_2$ (Liu and Ames, 1998). The second high-affinity system is the lysine-arginine-ornithine (LAO)-binding protein, ArgT (K_m for histidine, ~ 1 μM), which makes use of the $HisQMP_2$ complex for substrate translocation. There are three low-affinity histidine transporters (K_m, ~ 100 μM) in *S. typhimurium*: the AroP permease (Ames and Roth, 1968) and two other uncharacterized systems. AroP is a secondary active carrier belonging to the Amino Acid-Polyamine-Organocation (APC) superfamily. Of particular note is that in *S. typhimurium* and other enteric bacteria the genes encoding the transporters are not colocalized with genes encoding the degradative enzymes.

Histidine utilization has also been investigated in differ- ent species of *Pseudomonas*, but primarily in *Pseudomo- nas putida* (George and Phillips, 1970; Itoh *et al*., 2007). However, the transport system(s) for histidine uptake remains uncharacterized, despite the recognition of a transporter-like gene embedded in the *hut* operon of *P. putida* (A. Phillips, pers. comm.). Recently, Rietsch and colleagues (2004) performed deletion analysis of a puta- tive transporter gene (PA5097) in the *hut* locus of *Pseudomonas aeruginosa* PAO1 in a study that was moti- vated by the regulation of type III secretion genes. The mutant was compromised in its ability to grow on histidine and the PA5097 gene was thus designated *hutT* (Rietsch *et al*., 2004). Notably, PA5097 is one of eight putative transporter genes encoded by the *hut* locus of *P. aerugi- nosa* PAO1 (Itoh *et al*., 2007).

Interestingly, many bacteria, including *P. fluorescens* SBW25, are able to utilize urocanate (imidazole-4-acrylic acid or urocanic acid) – the first intermediate of the *hut* pathway – as the sole source of carbon and/or nitrogen (Hug *et al*., 1999; Rico and Preston, 2008). Urocanate is the direct inducer of the *hut* operon and urocanate (not histidine) is capable of binding the HutC repressor causing HutC to dissociate from the operator site. However, for strains unable to utilize urocanate, external urocanate is a poor inducer of *hut* gene expression owing to its inability to penetrate the cell (Brill and Magasanik, 1969; Hu *et al*., 1987). These data suggest the existence of a urocanate transporter although the identity of any such transporter remains to be determined.

Our study began with analysis of the capacity of 164 plant-colonizing *Pseudomonas* strains to utilize histidine or urocanate for growth. Finding polymorphism we per- formed an *in silico* analysis of the *hut* locus from 17 available genome-sequenced *Pseudomonas* and found high conservation of metabolic enzymes, but poor conser- vation among putative transporters. This led to a detailed characterization of five putative transport genes in the *hut* locus of *P. fluorescens* SBW25, which showed presence of two histidine uptake systems, and one dedicated to the uptake of urocanate. In many instances, transfer of the SBW25-derived histidine and urocanate transporters into natural isolates unable to utilize one or other of the substrates complemented the defects. The histidine/urocanate polymorphism is thus attributable to genetic differences in transport systems. Finally, our discovery of urocanate-specific transport genes draws attention to the availability and ecological significance of urocanate in natural environments.

Results

Utilization of histidine and urocanate by plant-associated Pseudomonas

Phenotypic diversity of leaf-colonizing *Pseudomonas* was assessed with a total of 164 strains isolated from the phyllosphere of sugar beets (*Beta vulgaris* var. Amethyst). Their ability to grow on histidine and separately on uro-canate was examined in M9 salt medium supplemented with histidine or urocanate. Absorbance (A_{450}) was deter-mined every 5 min over a period of 48 h. With the assis-tance of visual inspection, strains with maximum absorbance values less than 0.3 were considered as His^- and/or Uro^-. Results, available in Table S1 and summa-rized in Fig. 2, revealed considerable variation of pheno-types. While most isolates could utilize both histidine and urocanate as growth substrates (His^+ Uro^+: 77.4%, 127 strains) the remaining isolates were comprised of types that could utilize either histidine, but not urocanate (His^+

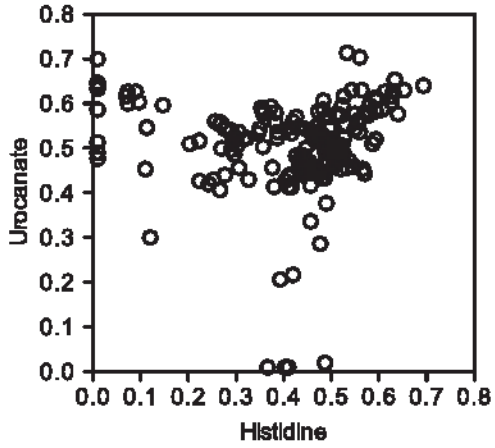

Fig. 2. Growth of *Pseudomonas* isolates on histidine versus urocanate as sole carbon and nitrogen sources. Data are mean values of three independent cultures in terms of maximum absorbance (A_{450}) over a growth period of 48 h. Error bars are omitted for clarity; coefficient of variation for the population is 3.5% for growth on histidine and 2.6% for growth on urocanate.

Uro$^-$: 4.9%, 8 strains) and vice versa (His$^-$ Uro$^+$: 17.7%, 29 strains). For the His$^+$ Uro$^+$ strains, there was a significant weak positive correlation between growth on histidine and urocanate in terms of maximum absorbance ($R = 0.4$, $P < 0.001$) and lag time ($R = 0.38$, $P < 0.001$), but no significant correlation on maximum growth rates ($R = 0.11$, $P = 0.23$).

Given that both histidine and urocanate are degraded by the same catabolic pathway, the finding that a significant number of *Pseudomonas* isolates (~ 23%) use one substrate, but not the other is of interest (refer to the His$^+$ Uro$^-$ and His$^-$ Uro$^+$ isolates). For an isolate capable of growth on histidine, it must harbour all the enzymes required for the bacterium to grow on urocanate; the fact that weak or no growth was observed on urocanate (His$^+$ Uro$^-$) suggests that the isolate lacks a functional transporter for urocanate. For strains that are phenotypi- cally His$^-$ Uro$^+$, there are two possible explanations: they lack either a functional histidine transporter or a func- tional histidase (HutH), the enzyme that converts histi- dine to urocanate, or both. We thus predicted that the observed phenotypic variation in terms of histidine and urocanate utilization is most likely attributable to genetic differences in transport systems. The hypothesis led to the detailed *in silico* and functional analysis of histidine- and urocanate-specific transporters in *Pseudomonas* (described below).

Genomic analysis of histidine transporters in the hut *loci of* Pseudomonas

In silico analysis of *hut* genes was first performed in *P. fluorescens* SBW25 and three transport systems are predicted in the *hut* locus (Fig. 1): two permeases (Pflu0362 and Pflu0368) and one ABC-type transporter (Pflu0363, Pflu0364 and Pflu0365). Details of the analysis are shown in Table 1.

The two permease genes (*pflu0362* and *pflu0368*) are of similar length and encode predicted proteins of 481 and 469 amino acids respectively. However, they share very little sequence identity to each other (14%). Computa- tional hydropathy analysis using the TMHMM Server (version 2.0) predicted 13 transmembrane domains for the deduced amino acid sequence of *pflu0362* and 12 transmembrane regions for the gene product of *pflu0368*. A search of the Conserved Domain Database (CDD) showed that Pflu0362 possesses the permease do- main for cytosine/purines, uracil, thiamine, allantoin (pfam02133, *E*-value: $4e^{-31}$), whereas Pflu0368 harbours the amino acid permease domain (pfam00324, $7e^{-57}$). A BlastP search of the transporter classification database (http://www.tcdb.org/) showed that Pflu0362 belongs to transporter class (TC) 2.A.39, the Nucleobase:Cation Symporter-1 (NCS1) family, whereas Pflu0368 is a member of the Amino Acid Polyamine Organocation (APC) Superfamily (TC: 2.A.3). Together the *in silico* analysis data suggested that *pflu0362* and *pflu0368* encode transporter proteins with functions that are unlikely to be redundant.

Genes encoding the putative ABC transporter system are organized by a gene order typical for ABC transport- ers involved in substrate uptake (Hosie and Poole, 2001): a periplasmic binding protein (Pflu0363) followed by a membrane-spanning domain (Pflu0364) and then an ATP-binding cassette (Pflu0365). The best homologues of the SBW25 genes among functionally characterized trans- porters are the HutXWV genes from the symbiotic soil-dwelling bacterium *Sinorhizobium meliloti* (Table 1). The *hutXWV* of *S. meliloti* encodes a functional histidine trans- porter, which is also involved in proline and betaine uptake (Boncompagni *et al*., 2000). For consistency, *pflu0363*, *0364* and *0365* are designated *hutXWV* on the basis of sequence similarities and the functional charac- terizations described below.

Comparative analysis of putative transporters located in the *hut* locus was performed between *P. fluorescens* SBW25 and 16 other genome-sequenced *Pseudomonas* strains that are currently available in the 'Pseudomonas Genome Database' (http://www.pseudomonas.com). All strains, except *Pseudomonas stutzeri* A1501, possess the *hut* metabolic genes, which are highly conserved and present only in single copies [with the exception of *hutH* (Zhang and Rainey, 2007a)]. Conversely, the analysis revealed polymorphism in histidine uptake components. For example, *P. putida*, possesses only one transport gene encoding a permease, while *P. aeruginosa*, pos- sesses eight putative transporter genes (Table 1). These

Table 1. Comparative analysis of putative transporters in the *hut* locus of *P. fluorescens* SBW25 and other *Pseudomonas* species.

Gene No.	Gene name	Predicted function	TMs	Best homologue in TCDB[a]	Sequence identity with homologue in the *hut* loci of other *Pseudomonas*		
					P. putida KT2440	*P. syringae* DC3000	*P. aeruginosa* PAO1[b]
Pflu0362	*hutT*$_u$	Permease	13 (481aa)	FCY2 (24%)	None	None	PA5099 (79%)
Pflu0363	*hutX*	Periplasmic binding Protein	0 (321aa)	HutX (45%)	None	PSPTO5271 (85%)	PA5096 (77%) PA5103 (51%)
Pflu0364	*hutW*	Integral membrane Component	7 (283aa)	HutW (61%)	None	PSPTO5272 (93%)	PA5095 (90%) PA5102 (19%)
Pflu0365	*hutV*	ATP-binding protein	0 (274aa)	HutV (67%)	None	PSPTO5273 (88%)	PA5094 (87%)
Pflu0368	*hutT*$_h$	Permease	12 (469aa)	ProY (55%)	PP5031 (86%)	PSPTO5276 (83%)	PA5097 (78%)

a. The purine-cytosine permease protein FCY2 of *Saccharomyces cerevisiae* (Weber *et al.*, 1990) and the proline-specific permease ProY of *Salmonella typhimurium* (Liao *et al.*, 1997) were derived from NCBI database with accession number of P17064 and P37460 respectively. HutXWV is a histidine ABC transport from *Sinorhizobium meliloti* that is also involved in proline and betaine uptake (AF111939) (Boncompagni *et al.*, 2000). Amino acid sequence identity is shown in parenthesis.
b. The *hut* locus of *P. aeruginosa* PAO1 contains an additional periplasmic substrate-binding protein (PA5101), which is not a homologue of HutX.

findings are consistent with our prediction of genetic variation in transport systems in natural *Pseudomonas* populations.

Deletion analysis of the predicted histidine transporters

Next we sought to identify histidine- and urocanate-specific transporters in *P. fluorescens* SBW25: SBW25 is capable of growth on both histidine and urocanate, suggesting the existence of efficient transport system(s) for these substrates. Transport systems dedicated to histi- dine and/or urocanate uptake are most likely present within the *hut* operon.

To test this hypothesis, each of the three putative transport systems (Δ*pflu0362*, Δ*pflu0368* and Δ*hutXWV*) was inactivated and ability of the mutants to grow on histidine and urocanate was determined. Results are listed in Table 2 and details of the growth curves are shown in Fig. 3. Strain PBR855 (Δ*pflu*0362) grew as wild type on histidine, but was unable to grow on urocanate; while PBR856 (Δ*pflu*0368) grew normally on urocanate but showed delayed growth on histidine (Table 2). Mutant PBR857 (Δ*hutXWV*) grew normally on both histidine and urocanate. These data, combined with *in silico* analysis, implicate *pflu0362* as a urocanate-specific transporter, and *pflu0368* as a histidine transporter: henceforth, *pflu0362* and *pflu0368* are designed *hutT*$_u$ and *hutT*$_h$, respectively, to denote their specificity for urocanate and histidine. No physiological function was defined for *hutXWV*.

To further confirm the assigned *hutT*$_u$ and *hutT*$_h$ functions, the coding regions of *hutT*$_u$ and *hutT*$_h$ were each cloned into the broad-host-range plasmid pME6010 [where they were expressed from a constitutive promoter (P_K)] to produce pME6010-*hutT*$_h$ or pME6010-*hutT*$_u$. These plasmids were introduced into PBR856 (Δ*hutT*$_h$) and pBR855 (Δ*hutT*$_u$), respectively, and the ability to grow on histidine and urocanate was examined (Table 2). The growth defects of pBR855 (Δ*hutT*$_u$) on urocanate and PBR856 (Δ*hutT*$_h$) on histidine were fully restored by pME6010-*hutT*$_u$ and pME6010-*hutT*$_h$ respectively. No cross-complementation was observed: strain PBR861 [Δ*hutT*$_u$ (pME6010-*hutT*$_h$)] was still unable to grow on urocanate; strain PBR863 [Δ*hutT*$_h$ (pME6010-*hutT*$_u$)] showed slow growth on histidine which is comparable to the growth of mutant PBR856 (Δ*hutT*$_h$).

The fact that PBR856 (Δ*hutT*$_h$) was not completely defective for growth on histidine prompted further investigation into the role of *hutXWV* (which we reasoned might have been responsible for the ability of the *hutT*$_h$ mutant to grow slowly on histidine). The *hutXWV* genes of PBR856 (Δ*hutT*$_h$) were therefore deleted and significantly, the double-deletion mutant PBR858 (Δ*hutXWVT*$_h$) showed slower growth on histidine as compared with Δ*hutT*$_h$ alone

Table 2. Phenotypes of mutant strains with deletion of the putative transporters.

		Growth as sole carbon and nitrogen sources	
Strain	Genotype	Histidine[a]	Urocanate
SBW25	Wild type	+	+
PBR855	Δ*hutT*$_u$	+	–
PBR856	Δ*hutT*$_h$	S	+
PBR857	Δ*hutXWV*	+	+
PBR858	Δ*hutT*$_h$*XWV*	S	+
PBR859	Δ*hutT*$_h$*T*$_u$*XWV*	S	–
PBR860	Δ*hutT*$_u$ (pME6010-*hutT*$_u$)	+	+
PBR861	Δ*hutT*$_u$ (pME6010-*hutT*$_h$)	+	–
PBR862	Δ*hutT*$_u$ (pME6010)	+	–
PBR863	Δ*hutT*$_h$ (pME6010-*hutT*$_u$)	S	+
PBR864	Δ*hutT*$_h$ (pME6010-*hutT*$_h$)	+	+
PBR865	Δ*hutT*$_h$ (pME6010)	S	+

a. S denotes slower growth with a longer lag phase when compared with the wild-type strain.

(Fig. 3): the lag phase was extended from 16.7 0.2 h for PBR856 (Δ*hutT*$_h$) to 18.4 0.2 h for PBR858 (Δ*hutXWVT*$_h$) and the maximum specific growth rate (μmax) was reduced from 0.195 0.005 h^{-1} for PBR856 (Δ*hutT*$_h$) to 0.171 0.004 h^{-1} for PBR858 (Δ*hutXWVT*$_h$). Furthermore, a mutant lacking all three putative transport systems was made by deleting the *hutT*$_u$ and *hutXWV* genes from PBR856 (Δ*hutT*$_h$). The resultant mutant strain PBR859 (Δ*hutT*$_u$*XWVT*$_h$) was unable to grow on urocanate (Uro$^-$) and its growth on histidine (lag time: 18.95 0.39 h; μmax: 0.174 0.004 h^{-1}) was comparable to mutant PBR858 (Δ*hutT*$_h$*XWV*) (Table 2), which confirmed the above finding that *hutT*$_u$ is not involved in histidine uptake. Taken together, these data implicate a role for *hutXWV* in histidine uptake but indicate the existence of additional histidine transporters elsewhere in the genome.

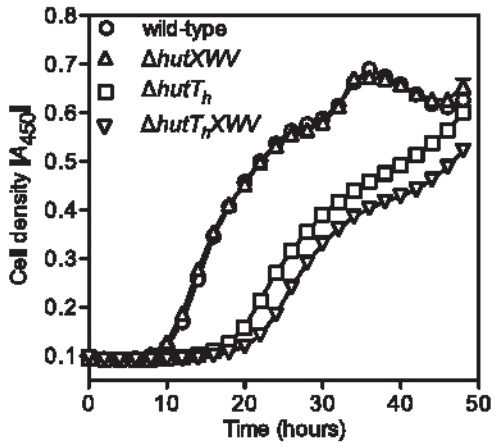

Fig. 3. Growth properties of *P. fluorescens* SBW25 and its derived mutants of putative transporter genes. Absorbance at the wavelength of 450 nm (A_{450}) was measured for cells grown in M9 salt medium supplemented with histidine (15 mM) as the sole source of carbon and nitrogen: wild-type SBW25 and mutants PBR856 (Δ*hutT*$_h$), PBR857 (Δ*hutXWV*) and PBR858 (Δ*hutT*$_h$*XWV*). Results are means and standard errors of six independent cultures.

To identify the predicted unknown transporter(s) we first performed a genome-wide search for homologues of the archetypical ABC-type histidine transport system that has been well characterized in *Salmonella typhimurium* (Liu and Ames, 1998). This led to the identification of two candidate loci: locus 1 (*pflu1311, 1310, 1309* and *1307*) and locus 2 (*pflu4765, 4764, 4763* and *4761*) with each harbouring four genes encoding potential homologues of *hisJ*, *Q*, *M* and *P* respectively. However, a mutant devoid of both loci and *hutT*$_h$*XWV* (strain PBR866) grew normally on histidine as the sole carbon and nitrogen source when compared with mutant PBR858 (Δ*hutT*$_h$*XWV*). This result demonstrates that the two putative HisJQMP homologues (Pflu1307-1311 and Pflu4761-4765) are not the high-throughput histidine transporters responsible for growth of the *hutT*$_h$*XWV* deletion strain (PBR858) on histidine. Next we performed an extensive transposon mutagenesis analysis for His$^-$ mutants, but no putative transporter genes were identified, except a transporter-like sensor kinase gene (*cbrA*) that is required for the transcriptional activation of *hut* (Zhang and Rainey, 2008). The hypoth- esis that the CbrA N-terminal domain functions in histidine transport has been the subject of further investigation and the results will be published separately.

HutT$_h$ *is the major high-affinity histidine transporter*

To further demonstrate the functional roles of the three transport systems (HutT$_h$, HutT$_u$ and HutXWV) in histidine uptake, wild-type SBW25 and the derived mutant strains were subjected to whole-cell histidine transport assays. Cell suspensions of wild-type SBW25 grown overnight in minimal salt medium supplemented with histidine (as the

sole carbon and nitrogen source) transported [^{3}H]histidine (1 μM) at a rate of 0.10 0.02 nmol min^{-1} (mg protein)$^{-1}$ (Fig. S1A). When the cells were pre-incubated with the protonophore CCCP, a compound that dissipates the proton motive force across the cell membrane, [^{3}H]histi- dine accumulation was abolished (Fig. S1A). These data show that accumulation of [^{3}H]histidine in wild-type cells is due to active transport and not caused by diffusion or non-specific binding of [^{3}H]histidine to the cells.

The rates of [^{3}H]histidine uptake by mutants PBR856 (Δ*hutT$_h$*), PBR855 (Δ*hutT$_u$*) and PBR857 (Δ*hutXWV*) were measured and compared with wild-type cells. The rates of [^{3}H]histidine uptake in cells of the wild type, PBR855 (Δ*hutT$_u$*) and PBR857 (Δ*hutXWV*) were 0.10 0.02, 0.11 0.02 and 0.12 0.03 nmol min^{-1} (mg protein)$^{-1}$ respectively. In contrast, the rate of [^{3}H]histidine transport in PBR856 (Δ*hutT$_h$*) was significantly reduced [0.03 0.01 nmol min^{-1} (mg protein)$^{-1}$], suggesting that HutT$_h$ is the major high-affinity histidine transporter. To validate this proposal, the kinetics of [^{3}H]histidine uptake in wild-type SBW25 and mutant PBR856 (Δ*hutT$_h$*) were determined over a range of external histidine concentrations (1-20 μM). Transport of [^{3}H]histidine into wild-type SBW25 followed Michaelis-Menten kinetics (Fig. S1B) with the apparent K_m and V_{max} values of 0.78 μM histidine and 0.66 nmol min^{-1} (mg protein)$^{-1}$ respectively (Fig. S1C). When these experiments were performed with PBR856 (Δ*hutT$_h$*), the rate of histidine transport was low [approximately 0.03 nmol min^{-1} (mg protein)$^{-1}$] and even at a concentration of 20 μM histidine no significant increase in the rate of uptake was noted (data not shown). When the rate of [^{3}H]histidine transport in PBR856 (Δ*hutT$_h$*) was measured at an external concentration of 2 mM, an uptake rate of 4.40 0.70 nmol min^{-1} (mg protein)$^{-1}$ was detected, suggesting that a permease with low affinity (non-saturable) was present in Δ*hutT$_h$* mutant cells.

The rates reported here for histidine transport, while comparable to those reported for amino acid transport in whole cells of *P. aeruginosa* (Kay and Gronlund, 1969; 1971), are lower than the rate of amino acid consumption required for growth. To determine if this was unique to histidine with *P. fluorescens* SBW25, we measured the transport of both [^{3}H]- and [^{14}C]-labelled amino acids at a final concentration of 5 μM. The rates of transport [nmol min^{-1} (mg protein)$^{-1}$] were in the same range as for histidine: 0.35 0.04 for [^{14}C]arginine; 0.42 0.02 for [^{14}C]serine; 0.50 0.08 for [^{3}H]histidine and 3.11 0.45 for [^{3}H]proline. Non-metabolizable radioactive histidine analogues were not available for the current study and therefore the absolute rate of histidine transport (i.e. in the absence of metabolism) cannot be measured with cer- tainty. However, the values determined for histidine uptake are sufficient for a relative comparison between the wild type and various *hut* transport mutants at low concentrations of histidine.

Diversity of histidine and urocanate utilization is attributable to variation in transporters

Armed with the knowledge of histidine- and urocanate-specific transporters (*hutT$_h$* and *hutT$_u$*) in *P. fluorescens* SBW25, we performed heterologous complementation to test the hypothesis of transporter deficiency in the natu- rally occurring His$^-$ or Uro$^-$ strains. Using the standard procedure of plasmid conjugation, pME6010-*hutT$_h$* was successfully introduced into 22 His$^-$ Uro$^+$ strains, pME6010-*hutT$_u$* into six His$^+$ Uro$^-$ strains. The vector pME6010 was also conjugated into those strains as a control. The purified transconjugants were then sub- jected to growth assays in minimal medium with histidine or urocanate as sole carbon and nitrogen sources. Results showed that introduction of *hutT$_u$* restored the ability of four His$^+$ Uro$^-$ strains to grow on urocanate (Fig. 4). All the His$^-$ Uro$^+$ strains, except strain U128, gained the ability to grow on histidine with the complementation of *hutT$_h$* (Fig. 4). For strain U128, the observation that *hutT$_h$* was unable to confer any growth advantage on histidine suggested that a functional *hutH* is missing in this strain. Consistent with this prediction, when both *hutT$_h$* and *hutH$_2$* from *P. fluorescens* SBW25 were introduced into strain U128, the resulting recombinant strain was able to grow on histidine (Fig. 5). Notably, introduction of *hutH$_2$* alone was not sufficient for U128 to grow on histidine (Fig. 5), indicating that U128 lacks both a functional histidase and a functional histi- dine transporter. Taken together, the data demonstrate polymorphism with respect to the histidine and urocan- ate transport systems.

Discussion

Phenotypic variation, with accompanying genetic basis, is a fundamental requirement for evolution by natural selec- tion. Although evidence of phenotypic variation in natural populations abounds, its genetic basis is rarely under- stood (Barton and Turelli, 1989; Flint and Mott, 2001). In this study we focused on a natural population of 164 *Pseudomonas* isolates that shows polymorphism in ability to grow on histidine and urocanate. *In silico* analyses of *hut* loci in 17 genome-sequenced *Pseudomonas* strains led to a prediction that this phenotypic polymorphism could be explained by presence/absence of functional transport systems. Subsequent identification of histidine- and urocanate-specific transporters in *P. fluorescens* SBW25, followed by studies of heterologous complemen- tation, showed the hypothesis to be correct.

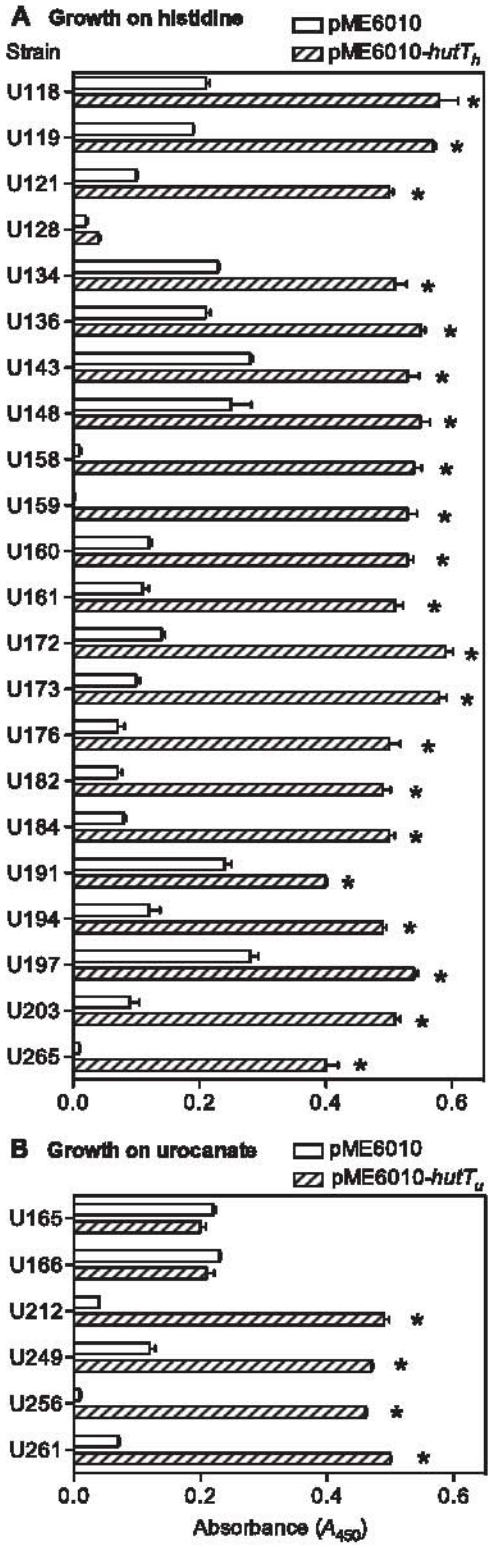

Fig. 4. Growth of His Uro strains on histidine (A) and His Uro strains on urocanate (B) after introduction of histidine- and urocanate-specific transporter genes ($hutT_h$ and $hutT_u$ respectively) from *P. fluorescens* SBW25. Maximum absorbance data (A_{450}) are means and standard errors of three independent cultures. Asterisks denote significant difference between strains with pME6010-$hutT_h$ (or pME6010-$hutT_u$) and the vector pME6010, as revealed by Student's *t*-test ($P < 0.05$).

characterized (McFall and Newman, 1996). *Pseudomo- nas fluorescens* SBW25 also possesses multiple systems for histidine uptake. $HutT_h$ is the major high-affinity histidine transporter, but our data show that *hutXWV* also plays a role in histidine transport. Data from both genetic and [^{3}H]histidine transport assays indicate that at least one additional low-affinity transporter system exists.

The complexity of histidine transport, which is also found with other amino acids, such as arginine (Caldara *et al*., 2007), can be partially explained by the multiple physiological roles of amino acids. Apart from being good sources of carbon and nitrogen, external histidine can be used directly for protein synthesis thus saving energy for anabolism. Moreover, histidine is energetically expensive to make, but for unknown reasons, there is a certain amount of leakage of intracellularly synthesized histidine from bacterial cells (Doige and Ames, 1993; Winkler, 1996). A high-affinity histidine transporter would allow the cell to recover external (leaked) histidine. It is interesting to note that *Escherichia coli* strains cannot grow on histi- dine due to the lack of degradative enzymes, but they do contain a functional histidine-specific transporter homolo- gous to the HisJQMP system of *S. typhimurium* (Caldara *et al*., 2007). Therefore, the multiple uptake systems are unlikely to be functionally redundant, but instead they may

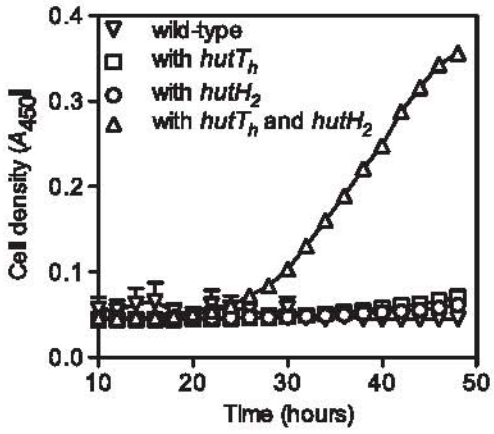

Fig. 5. Growth of *Pseudomonas* isolate U128 and its derived strains in minimal medium with histidine as sole carbon and nitrogen sources. Data are means and standard errors of six independent cultures: U128 with SBW25 $hutT_h$ (strain PBR867), U128 with SBW25 $hutH_2$ (strain PBR868) and U128 with both $hutT_h$ and $hutH_2$ (strain PBR869).

A multiplicity of histidine transporters has been well documented in *S. typhimurium*, where at least five systems are capable of transporting histidine; however, only three systems (HisJQMP, ArgT and AroP) have been

act in a cooperative manner to ensure efficient transport of histidine from extremely low to high concentrations.

In contrast to the complexity of histidine transporters in SBW25, urocanate uptake appears to be mediated by a single transporter protein $HutT_u$. The first two steps of the *hut* pathway, which produces urocanate from histidine [catalysed by histidase (HutH)] and degrades urocanate to imidazolone propionate [IPA, catalysed by urocanase (HutU)], are highly conserved from bacteria to humans (Itoh *et al*., 2007; Zhang and Rainey, 2007a). Therefore, urocanate is not a substrate that is normally expected in natural environments. Surprisingly, as shown in this work, certain bacterial strains have specific urocanate transport systems that confer ability to utilize urocanate as a carbon and nitrogen source. Such a finding leads to a hypothesis that urocanate is found in natural environments.

Indeed, urocanate is accumulated in the human stratum corneum, due to the absence of urocanase activity in the skin (Decara *et al*., 2008; Gibbs and Norval, 2011). The endogenously produced *trans*-urocanate acts as a 'natural sunscreen' to absorb ultraviolet (UV) light energy via a reaction of photoisomerization and the resultant *cis*-urocanate is involved in UV-induced photoimmuno- suppression with a consequent role in photocarcinogen- esis (Barresi *et al*., 2011). Nevertheless, urocanate produced in the stratum corneum is excreted through sweat and potentially serves bacteria as a significant source of carbon and nitrogen. Not surprisingly then, some prokaryotic members of the epidermal microflora are capable of utilizing *trans*- and/or *cis*-urocanate (Hug *et al*., 1999). However, *Pseudomonas* strains are not typical members of the human epidermal flora, so urocan- ate produced in the stratum corneum does not provide a plausible explanation for the presence of urocanate- utilizing ability in saprophytic *Pseudomonas*.

One potential source of urocanate for *Pseudomonas* may be fungi. A study of histidine catabolism in *Aspergil- lus nidulans* showed that histidine can be used as a source of nitrogen, but not a source of carbon (Polking- horne and Hynes, 1982) - one molecule of ammonia is produced when histidine is converted to urocanate. When grown under laboratory conditions, *A. nidulans* does not express urocanase activity and consequently, urocanate is accumulated and secreted into the medium.

Little is known about the possible developmental regulation of urocanase in plants, except a single report regarding the cloning of a urocanase gene from white clover (*Trifolium repens*) (Koberstaedt *et al*., 1992). Our finding that urocanate utilization is common among plant- associated *Pseudomonas* implicates either the plant, or other microbes growing in association with plants, as the source of this nutrient. None of the 164 leaf-colonizing *Pseudomonas* was able to grow on *cis*-urocanate (data not shown), which suggests that plants are not producing this compound as a means of photoprotection.

Patterns of nutrient utilization are important descriptors of physiological capability and have a long history of use in numerical taxonomic analysis of bacterial species (Garrity, 2005). A useful tool for rapid identification of Gram-negative bacteria is the Biolog GN2 MicroPlate, which assesses the ability of a bacterial strain to utilize a panel of 95 different carbon sources, including histidine and urocanate. The usefulness of nutrient phenotypes in bacterial classification suggests that the pattern of nutri- ent utilization is a result of natural selection that reflects nutrient availability in the natural environment. It is there- fore of interest to understand the genetic bases.

Our work here shows that variation in the capacity to utilize histidine and urocanate - a polymorphic trait - is due to variation in the uptake systems (transporters) and not variation in catabolic genes. While a seemingly sur- prising finding, it does sit in accord with both theoretical and experimental studies which show that fitness improvements are likely to occur via changes in uptake systems, as opposed to changes in core metabolic enzymes (Dykhuizen *et al*., 1987; Dean, 1995). Explain- ing the ecological causes for this variation is the next step. While it is possible that variation is due to drift, it seems more likely to reflect the hand of selection - a consequence of variation in the patchiness of histidine and urocanate on the plant surfaces. One possibility is that the polymorphism arises from prolonged selection in an environment lacking either histidine or urocanate. Under such conditions mutations in genes of the *hut* pathway would be neutral. However, a shift back to an environment with histidine or urocanate could, if a muta- tion has inactivated a catabolic enzyme, result in the build up of a non-metabolizable intermediate. The del- eterious effects on the cell may select for mutations in one or more of the transporters.

Experimental procedures

Bacterial strains, plasmids and growing conditions

Ancestral *P. fluorescens* SBW25 was isolated in 1989 from the leaf surface of a sugar beet plant grown at the University of Oxford farm, Wytham, Oxford, UK (Bailey *et al*., 1995). In 1993, a total of 164 *Pseudomonas* strains were isolated from the phyllosphere of sugar beets grown in the same area of Oxford as previously described (Rainey *et al*., 1994). Some of the 164 strains (108 isolates) were subjected to a previous multi-locus enzyme electrophoresis (MLEE) analysis wherein details of the sampling are provided (Haubold and Rainey, 1996).

Escherichia coli DH5$\alpha\lambda_{pir}$ was used for gene cloning and subsequent conjugation into *Pseudomonas* (Zhang *et al*., 2004). Both *Pseudomonas* and *E. coli* strains (Table 3) were routinely grown in Luria - Bertani medium (LB) at 28°C and

Table 3. Bacterial strains and plasmids used in this study.

Strain and plasmid	Genotypes and relevant characteristics	Reference or application
P. fluorescens		
SBW25	Wild-type strain isolated from sugar beet	Bailey *et al*. (1995)
PBR866	SBW25Δ*hutT$_h$XWV* Δ*pflu1309-1311* Δ*pflu4763-4765*	This work
U128	Wild-type strain isolated from sugar beet	Haubold and Rainey (1996)
PBR867	U128 (pME6010-*hutT$_h$*)	This work
PBR868	U128::Tn*7*-*hutH$_2$*	This work
PBR869	U128::Tn*7*-*hutH$_2$* (pME6010-*hutT$_h$*)	This work
Plasmid		
pRK2013	Helper plasmid, Tra$^+$, Km^R	Ditta *et al*. (1980)
pUIC3	Integration vector with promoterless *'lacZ*, Mob$^+$, Tc^R	Rainey (1999)
pME6010	Shuttle vector for gene expression, Tc^R	Heeb *et al*. (2000)
pUIC3-51	Delivery plasmid for *hutT$_u$* deletion, Tc^R	This work
pUIC3-58	Delivery plasmid for *hutT$_h$* deletion, Tc^R	This work
pUIC3-21	Delivery plasmid for *hutT$_u$XWV* deletion, Tc^R	This work
pUIC3-116	Delivery plasmid for *hutXWV* deletion, Tc^R	This work
pUC18T-mini-Tn*7*T-Gm-LAC	A Tn*7*-based cloning vector for gene expression, Gm^R	Choi *et al*. (2005)
pUX-BF13	Helper plasmid for transposition of the Tn*7* element, Ap^R	Bao *et al*. (1991)
pTn*7*-*hutH$_2$*	pUC18T-mini-Tn*7*T-Gm-LAC with SBW25 *hutH$_2$*, Gm^R	This work
pME6010-*hutT$_h$*	The coding region of SBW25 *hutT$_h$* cloned into pME6010 The	This work
pME6010-*hutT$_u$*	coding region of SBW25 *hutT$_u$* cloned into pME6010	This work

37°C respectively. Where indicated, *Pseudomonas* strains were also cultivated in M9 salts medium (MSM) supple- mented with glucose (0.4%) and ammonium chloride (1 g l^{-1}). Histidine or urocanate (*trans*-isoform) was purchased from Sigma-Aldrich and supplemented as the sole source of carbon and nitrogen at the final concentration of 15 mM. Growth of *Pseudomonas* strains was assessed by using a VersaMax microtitre plate reader (Molecular Devices) as described previously (Zhang and Rainey, 2007a).

Construction of Pseudomonas *mutant strains and genetic complementation*

Standard recombinant DNA techniques were used following manufacturers' recommendations. PCR was performed using DNA polymerase from Invitrogen (Auckland, New Zealand). Oligonucleotide primers used in this work are available in Table S2. Gene mutation was achieved by a previously described procedure of SOE-PCR (Horton *et al*., 1989; Zhang and Rainey, 2007b) in conjunction with a two-step allelic exchange strategy, using the suicide integration vector pUIC3.

Heterologous complementation with the histidine and uro- canate transporter genes from *P. fluorescens* SBW25 was performed by cloning PCR-amplified coding region of *hutT$_h$* or *hutT$_u$* into pME6010 at the EcoRI site (Heeb *et al*., 2000). The resultant recombinant plasmids were mobilized into the envi- ronmental *Pseudomonas* isolates by conjugation with the help of pRK2013 (Tra$^+$). The coding region of SBW25 *hutH$_2$* was previously cloned into the EcoRI site of pME6010 (Zhang and Rainey, 2007a). To facilitate complementation of both *hutT$_h$* and *hutH$_2$*, the *hutH$_2$* fragment was retrieved from pME6010-*hutH$_2$* by BglII/HindIII digestion and cloned into the Tn*7*-based vector pUC18T-mini-Tn*7*T-Gm-LAC, which was treated with BamHI/HindIII. The resulting plasmid was conju- gated into *Pseudomonas* with the help of pUX-BF13 and pRK2013 (Choi *et al*., 2005). The Tn*7* element carrying *hutH$_2$* gene was integrated into the unique chromosome site, which was confirmed by PCR using primers SBW25-glmS and Tn*7*R109 (Lambertsen *et al*., 2004).

Transport assays

Exponentially growing cells from 25 ml of culture were har- vested by centrifugation (7000 *g*, 10 min, 4°C) and washed twice in 50 mM potassium phosphate buffer containing 2 mM magnesium chloride (pH 7.2, 4°C). Cells (200 μl aliquots) were then suspended in the same buffer to a density of 1.0-1.5 (OD_{600}), and the cells energized (for 10-15 min) with the addition of glucose (10 mM). To initiate transport, 10 μl of L-[2,5-^{3}H]histidine (1.74 TBq mmol^{-1}) was added to the cell suspension to achieve a final concentration of 1 μM (3700 Bq). Other amino acids used in this study were: L-[U-^{14}C]serine (5.59 GBq mmol^{-1}), L-[U-^{14}C]arginine (12.9 GBq mmol^{-1}), L-[2,3,4,5-^{3}H]proline (2.78 TBq mmol^{-1}) at the con- centration indicated in the text. After various time intervals, transport was terminated by the addition of 2 ml of ice-cold LiCl (100 mM) and rapid filtration through cellulose-nitrate filters (0.45 μm pore size). The filters were washed again with 2 ml of LiCl, dried, and counts per min (CPM) were deter- mined using an LKB Wallac 1214 Rackbeta liquid scintillation counter. Where initial rates of transport are reported, the rate was determined between 0 and 40 s and was first order with respect to protein concentration. Protein content of each cell suspension was determined by using the bicinchoninic acid (BCA) protein assay kit from Sigma-Aldrich, with bovine serum albumin as the standard. For the protein assay, cells were lysed with 1 M NaOH and incubated at 95°C for 10 min. The cell lysate was neutralized with 1 M HCl prior to assay. Metabolic inhibitors, tested as potential inhibitors of histidine uptake, were added to the transport assay medium 15 min prior to [^{3}H]histidine addition at the final concentrations indi- cated in the text. All water-insoluble inhibitors were dissolved in 95% ethanol and compared with ethanol-treated controls.

Acknowledgements

We thank David Hsiao and Annabel Gunn for technical assistance. This work was supported by the Marsden Fund Council from Government funding administered by the Royal Society of New Zealand. P.B.R. is a James Cook Research Fellow.

References

Ames, G.F. (1985) The histidine transport system of *Salmonella typhimurium*. *Curr Top Membr Trans* **23:** 103-119.

Ames, G.F., and Roth, J.R. (1968) Histidine and aromatic permeases of *Salmonella typhimurim*. *J Bacteriol* **96:** 1742-1749.

Ames, G.F., Noel, K.D., Taber, H., Spudich, E.N., Nikaido, K., and Afong, J. (1977) Fine-structure map of the histidine transport genes in *Salmonella typhimurium*. *J Bacteriol* **129:** 1289-1297.

Bailey, M.J., Lilley, A.K., Thompson, I.P., Rainey, P.B., and Ellis, R.J. (1995) Site directed chromosomal marking of a fluorescent pseudomonad isolated from the phytosphere of sugar beet; stability and potential for marker gene transfer. *Mol Ecol* **4:** 755-763.

Bao, Y., Lies, D.P., Fu, H., and Roberts, G.P. (1991) An improved Tn*7*-based system for the single-copy insertion of cloned genes into chromosomes of gram-negative bacte- ria. *Gene* **109:** 167-168.

Barresi, C., Stremnitzer, C., Mlitz, V., Kezic, S., Kammeyer, A., Ghannadan, M., *et al*. (2011) Increased sensitivity of histidinemic mice to UVB radiation suggests a crucial role of endogenous urocanic acid in photoprotection. *J Invest Dermatol* **131:** 188-194.

Barton, N.H., and Turelli, M. (1989) Evolutionary quantitative genetics: how little do we know? *Annu Rev Genet* **23:** 337-370.

Boncompagni, E., Dupont, L., Mignot, T., Osteras, M., Lambert, A., Poggi, M.C., and Le Rudulier, D. (2000) Characterization of a *Sinorhizobium meliloti* ATP-binding cassette histidine transporter also involved in betaine and proline uptake. *J Bacteriol* **182:** 3717-3725.

Brill, W.J., and Magasanik, B. (1969) Genetic and metabolic control of histidase and urocanase in *Salmonella typhimurium*, strain 15-59. *J Biol Chem* **244:** 5392-5402.

Caldara, M., Minh, P.N., Bostoen, S., Massant, J., and Charlier, D. (2007) ArgR-dependent repression of arginine and histidine transport genes in *Escherichia coli* K-12. *J Mol Biol* **373:** 251-267.

Choi, K.H., Gaynor, J.B., White, K.G., Lopez, C., Bosio, C.M., Karkhoff-Schweizer, R.R., and Schweizer, H.P. (2005) A Tn*7*-based broad-range bacterial cloning and expression system. *Nat Methods* **2:** 443-448.

Dean, A.M. (1995) A molecular investigation of genotype by environment interactions. *Genetics* **139:** 19-33.

Decara, J.M., Aguilera, J., Abdala, R., Sanchez, P., Figueroa, F.L., and Herrera, E. (2008) Screening of urocanic acid isomers in human basal and squamous cell carcinoma tumors compared with tumor periphery and healthy skin. *Exp Dermatol* **17:** 806-812.

Ditta, G., Stanfield, S., Corbin, D., and Helinski, D.R. (1980) Broad host range DNA cloning system for gram-negative bacteria: construction of a gene bank of *Rhizobium meliloti*. *Proc Natl Acad Sci USA* **77:** 7347-7351.

Doige, C.A., and Ames, G.F. (1993) ATP-dependent transport systems in bacteria and humans: relevance to cystic fibro- sis and multidrug resistance. *Annu Rev Microbiol* **47:** 291- 319.

Dykhuizen, D.E., Dean, A.M., and Hartl, D.L. (1987) Metabolic flux and fitness. *Genetics* **115:** 25-31.

Flint, J., and Mott, R. (2001) Finding the molecular basis of quantitative traits: successes and pitfalls. *Nat Rev Genet* **2:** 437-445.

Garrity, G.M. (2005) *Bergey's Manual of Systematic Bacteriology*. New York, USA: Springer.

George, D.J., and Phillips, A.T. (1970) Identification of alpha-ketobutyrate as the prosthetic group of urocanase from *Pseudomonas putida*. *J Biol Chem* **245:** 528-537.

Gibbs, N.K., and Norval, M. (2011) Urocanic acid in the skin: a mixed blessing? *J Invest Dermatol* **131:** 14-17.

Haubold, B., and Rainey, P.B. (1996) Genetic and ecotypic structure of a fluorescent *Pseudomonas* population. *Mol Ecol* **5:** 747-761.

Heeb, S., Itoh, Y., Nishijyo, T., Schnider, U., Keel, C., Wade, J., *et al*. (2000) Small, stable shuttle vectors based on the minimal pVS1 replicon for use in gram-negative, plant-associated bacteria. *Mol Plant Microbe Interact* **13:** 232- 237.

Horton, R.M., Hunt, H.D., Ho, S.N., Pullen, J.K., and Pease, L.R. (1989) Engineering hybrid genes without the use of restriction enzymes: gene splicing by overlap extension. *Gene* **77:** 61-68.

Hosie, A.H., and Poole, P.S. (2001) Bacterial ABC transporters of amino acids. *Res Microbiol* **152:** 259-270.

Hu, L., Mulfinger, L.M., and Phillips, A.T. (1987) Purification and properties of formylglutamate amidohydrolase from *Pseudomonas putida*. *J Bacteriol* **169:** 4696-4702.

Hug, D.H., Dunkerson, D.D., and Hunter, J.K. (1999) The degradation of L-histidine and *trans*- and *cis*-urocanic acid by bacteria from skin and the role of bacterial *cis*-urocanic acid isomerase. *J Photochem Photobiol B* **50:** 66-73.

Itoh, Y., Nishijyo, T., and Nakada, Y. (2007) Histidine catabolism and catabolite regulation. In *Pseudomonas*. Ramos, H.-L., and Fillous, A. (eds). Berlin, Germany: Springer, pp. 371-395.

Kay, W.W., and Gronlund, A.F. (1969) Amino acid transport in *Pseudomonas aeruginosa*. *J Bacteriol* **97:** 273-281.

Kay, W.W., and Gronlund, A.F. (1971) Transport of aromatic amino acids by *Pseudomonas aeruginosa*. *J Bacteriol* **105:** 1039-1046.

Koberstaedt, A., Lenz, M., and Retey, J. (1992) Isolation, sequencing and expression in *E. coli* of the urocanase gene from white clover (*Trifolium repens*). *FEBS Lett* **311:** 206-208.

Lambertsen, L., Sternberg, C., and Molin, S. (2004) Mini-Tn*7* transposons for site-specific tagging of bacteria with fluorescent proteins. *Environ Microbiol* **6:** 726-732.

Liao, M.K., Gort, S., and Maloy, S. (1997) A cryptic proline permease in *Salmonella typhimurium*. *Microbiology* **143:** 2903-2911.

Liu, P.Q., and Ames, G.F. (1998) *In vitro* disassembly and reassembly of an ABC transporter, the histidine permease. *Proc Natl Acad Sci USA* **95:** 3495-3500.

McFall, E., and Newman, E.B. (1996) Amino acids as carbon sources. In Escherichia coli *and* Salmonella: *Cellular and Molecular Biology*. Neidhardt, F.C. (ed.). Washington, DC, USA: ASM Press, pp. 358-379.

Phillips, D.A., Fox, T.C., King, M.D., Bhuvaneswari, T.V., and Teuber, L.R. (2004) Microbial products trigger amino acid exudation from plant roots. *Plant Physiol* **136:** 2887- 2894.

Polkinghorne, M.A., and Hynes, M.J. (1982) L-histidine utilization in *Aspergillus nidulans*. *J Bacteriol* **149:** 931- 940.

Rainey, P. (1999) Adaptation of *Pseudomonas fluorescens* to the plant rhizosphere. *Environ Microbiol* **1:** 243-257.

Rainey, P.B., Bailey, M.J., and Thompson, I.P. (1994) Phenotypic and genotypic diversity of fluorescent pseudomonads isolated from field-grown sugar beet. *Microbiology* **140:** 2315-2331.

Rediers, H., Rainey, P.B., Vanderleyden, J., and De Mot, R. (2005) Unraveling the secret lives of bacteria: use of *in vivo* expression technology and differential fluorescence induc- tion promoter traps as tools for exploring niche-specific gene expression. *Microbiol Mol Biol Rev* **69:** 217-261.

Rico, A., and Preston, G.M. (2008) *Pseudomonas syringae* pv. *tomato* DC3000 uses constitutive and apoplast-induced nutrient assimilation pathways to catabolize nutrients that are abundant in the tomato apoplast. *Mol Plant Microbe Interact* **21:** 269-282.

Rietsch, A., Wolfgang, M.C., and Mekalanos, J.J. (2004) Effect of metabolic imbalance on expression of type III secretion genes in *Pseudomonas aeruginosa*. *Infect Immun* **72:** 1383-1390.

Simons, M., Permentier, H.P., de Weger, L.A., Wijffelman, C.A., and Lugtenberg, B.J.J. (1997) Amino acid synthesis is necessary for tomato root colonization by *Pseudomonas fluorescens* strain WCS365. *Mol Plant Microbe Interact* **10:** 102-106.

Weber, E., Rodriguez, C., Chevallier, M.R., and Jund, R. (1990) The purine-cytosine permease gene of *Saccharomyces cerevisiae*: primary structure and deduced protein sequence of the FCY2 gene product. *Mol Microbiol* **4:** 585-596.

Wiedmann, M., Weilmeier, D., Dineen, S.S., Ralyea, R., and Boor, K.J. (2000) Molecular and phenotypic characteriza- tion of *Pseudomonas* spp. isolated from milk. *Appl Environ Microbiol* **66:** 2085-2095.

Winkler, M.E. (1996) Biosynthesis of histidine. In Escherichia coli *and* Salmonella: *Cellular and Molecular Biology*. Neidhardt, F.C. (ed.). Washington, DC, USA: ASM Press, pp. 485-505.

Zhang, X.X., and Rainey, P.B. (2007a) Genetic analysis of the histidine utilization (*hut*) genes in *Pseudomonas fluore- scens* SBW25. *Genetics* **176:** 2165-2176.

Zhang, X.X., and Rainey, P.B. (2007b) Construction and validation of a neutrally-marked strain of *Pseudomonas fluorescens* SBW25. *J Microbiol Methods* **71:** 78-81.

Zhang, X.X., and Rainey, P.B. (2008) Dual involvement of CbrAB and NtrBC in the regulation of histidine utilization in *Pseudomonas fluorescens* SBW25. *Genetics* **178:** 185- 195.

Zhang, X.X., Lilley, A.K., Bailey, M.J., and Rainey, P.B. (2004) Functional and phylogenetic analysis of a plant-inducible oligoribonuclease (*orn*) gene from an indigenous *Pseudomonas* plasmid. *Microbiology* **150:** 2889-2898.

Zhang, X.X., George, A., Bailey, M.J., and Rainey, P.B. (2006) The histidine utilization (*hut*) genes of *Pseudomo- nas fluorescens* SBW25 are active on plant surfaces, but are not required for competitive colonization of sugar beet seedlings. *Microbiology* **152:** 1867-1875.

Zhang, X.X., Liu, Y.H., and Rainey, P.B. (2010) CbrAB-dependent regulation of *pcnB*, a poly(A) polymerase gene involved in polyadenylation of RNA in *Pseudomonas fluorescens*. *Environ Microbiol* **12:** 1674-1683.

Supporting information

Additional Supporting Information may be found in the online version of this article:

Fig. S1. Uptake of [^{3}H]histidine by wild-type *P. fluorescens* SBW25.

A. Accumulation of radioactive histidine (^{3}H, 3700 Bq, 1 μM final concentration) in whole cells of SBW25 over time (closed squares). Additionally, [^{3}H]histidine uptake was also measured in cells that were pre-incubated in either 100 μM CCCP (closed triangles) or an equivalent volume of ethanol (closed circles).

B. Kinetics of histidine transport by SBW25 cells growing in minimal medium with histidine (15 mM) as the sole carbon and nitrogen sources. The initial uptake rates of histidine, expressed as nmoles of [^{3}H]histidine per minute per milligram of SBW25 protein, were measured over 40 s at varying concentrations of histidine from 1 μM to 20 μM.

C. Lineweaver-Burk plots of the data presented in (B). Experiments were performed two or more times and the values reported are the means of biological duplicates and the experimental error associated with these values is shown.

Table S1. Utilization of histidine or urocanate by *Pseudomo- nas* strains isolated from Oxford (UK).

Table S2. Oligonucleotide primers used in this work.

Please note: Wiley-Blackwell are not responsible for the content or functionality of any supporting materials supplied by the authors. Any queries (other than missing material) should be directed to the corresponding author for the article.

References

Adiri, R. S., U. Gophna, and E. Z. Ron. 2003. Multilocus sequence typing (MLST) of Escherichia coli O78 strains. FEMS Microbiology Letters 222:199-203.

Allison, S. L., and A. T. Phillips. 1990. Nucleotide sequence of the gene encoding the repressor for the histidine utilization genes of Pseudomonas putida. Journal of Bacteriology 172:5470-5476.

Barton, N. H., and M. Turelli. 1989. Evolutionary quantitative genetics: how little do we know? Annual Review of Genetics 23:337-370.

Bertani, G. 1951. Studies on lysogenesis. I. The mode of phage liberation by lysogenic Escherichia coli. Journal of Baceteriology 62:293-300.

Chan, M.-S., M. C. J. Maiden, and B. G. Spratt. 2001. Database-driven Multi Locus Sequence Typing (MLST) of bacterial pathogens Bioinformatics 17:1077-1083.

Choi, K.-H., J. B. Gaynor, K. G. White, C. Lopez, C. M. Bosio, R. R. Karkhoff-Schweizer, and H. P. Schweizer. 2005. a Tn7-based broad-range bacterial cloning and expression system. Nature Methods 2:443-448.

Consevage, M. W., R. D. Porter, and A. T. Phillips. 1985. Cloning and expression in Escherichia coli of histidine utilization genes from Pseudomonas putida. Journal of Bacteriology 162:138-146.

Cook, R. J. 2001. Disruption of histidine catabolism in NEUT2 mice. Archives of Biochemistry and Biophysics 392:226-232.

Coote, J. G., and H. Hassall. 1973. The degradation of L-histidine, imidazolyl-L-lactate and imidazolylpropionate by Pseudomonas testosteroni. Journal of Biochemistry 132:409-422.

Fernandez, R. F., E. Dolghih, and D. A. Kunz. 2004. Enzymatic assimilation of cyanide via pterin-dependent oxygenolytic cleavage to ammonia and formate in Pseudomonas fluorescens. Applied Environmental Microbiology 70:121-128.

Figurski, D. H., and D. R. Helinski. 1979. Replication of an origin-containing derivative of plasmid RK2 dependent on a plasmid function provided in trans. Proceedings of National Academy of Sciences USA 76:1648-1652.

Flint, J., and R. Mott. 2001. Finding the molecular basis of quantitative traits: successes and pitfalls. Nature Reviews Genetics 2:437-445.

George, D. J., and A. T. Phillips. 1970. Identification of a-ketobutyrate as the prosthetic group of urocanase from Pseudomonas putida. Journal of Biological Chemistry 245:528-537.

Haubold, B., and P. B. Rainey. 1996. Genetic and ecotypic structure of a fluorescent Pseudomonas population. Molecular Ecology 5:747-761.

Hernandez, D., J. G. Stroh, and A. T. Phillips. 1993. Identification of Ser143 as the site of modification in the active site of histidine ammonia-lyase. Archives of Biochemistry and Biophysics 307:126-132.

Hu, L., S. L. Allison, and A. T. Phillips. 1989. Identification of multiple repressor recognition sites in the hut system of Pseudomonas putida. Journal of Bacteriology 171:4189-4195.

Hu, L., and A. T. Phillips. 1988. Organization and multiple regulation of histidine utilization genes in Pseudomonas putida. Journal of Bacteriology 170:4272-4279.

Hug, D. H., D. D. Dunkerson, and J. K. Hunter. 1999. The degradation of L-histidine and trans- and cis-urocanaic acid by bacteria from skin and the role of bacterial cis-urocanic acid isomerase. Journal of Photochemistry and Photobiology 50:66-73.

Hug, D. H., D. Roth, and J. Hunter. 1968. Regulation of histidine catabolism by succinate in Pseudomonas putida. Journal of Bacteriology 96:396-402.

Itoh, Y., T. Nishijyo, and Y. Nakada. 2007. Histidine Catabolism and Catabolite Regulation. Springer Netherlands:371-395.

Joardar, V., M. Lindeberg, R. W. Jackson, J. Selengut, R. Dodson, L. M. Brinkac, S. C. Daugherty, R. DeBoy, A. S. Durkin, M. G. Giglio, R. Madupu, W. C. Nelson, M. J. Rosovitz, S. Sullivan, J. Crabtree, T. Creasy, T. Davidsen, D. H. Haft, N. Zafar, L. Zhou, R. Halpin, T. Holley, H. Khouri, T. Feldblyum, O. White, C. M. Fraser, A. K. Chatterjee, S. Cartinhour, D. J. Schneider, J. Mansfield, A. Collmer, and C. R. Buell. 2005. Whole-genome sequence analysis of Pseudomonas syringae pv.phaseolicola 1448A reveals divergence among pathovars in genes involved in virulence and transposition. Journal of Baceteriology 187:6488-6498.

Kammeyer, A. M., S. Pavel, S. S. Asghar, J. D. Bos, and M. B. M. Teunissen. 1997. Prolonged increase of cis-urocanic acid levels in human skin and urine after single total-body ultraviolet exposures. Jonrnal of Photochemistry and Photobiology 65:593-598.

Kannan, K., L. Kamala, S. Janiyani, M. Shivaji, and K. Ray. 1998. Histidine utilisation operon (hut) is upregulated at low temperature in the antarctic psychrotrophic bacterium Pseudomonas syringae. FEMS Microbiology Letters 161:7-14.

Kavanagh, G., J. Crosby, and M. Norval. 1995. Urocanic acid isomers in human skin: analysis of site variation. The British Journal of Dermatology 133:728-731.

Kessler, D., J. Re´tey, and G. E. Schulz. 2004. Structure and action of urocanase. Journal of Molecular Biology 342:183-194.

Khan, N. H., M. Ahsan, S. Yoshizawa, S. Hosoya, A. Yokota, and K. Kogure. 2008. Multilocus sequence typing and phylogenetic analyses of Pseudomonas aeruginosa Isolates from the ocean. Applied and Environmental Microbiology 74:6194-6205.

Liman, E. R. 2006. Use it or lose it: molecular evolution of sensory signaling in primates. European Journal of Physiology 453:125-131.

Lynch, M., and W. Gabriel. 1987. Environmental tolerance. The American Naturalist 129:282-303.

MacLean, R. C., G. Bell, and P. B. Rainey. 2004. The evolution of a pleiotropic fitness tradeoff in Pseudomonas fluorescens. Proceedings of National Academy of Sciences USA 101:8072-8077.

Maiden, M. C. J., J. A. Bygraves, E. Feil, G. Morelli, J. E. Russell, R. Urwin, Q. Zhang, J. Zhou, K. Zurth, D. A. Caugant, I. M. Feavers, M. Achtman, and B. G. Spratt. 1998. Multilocus sequence typing: A portable approach to the identification of clones within populations of pathogenic microorganisms. Proceedings of National Academy of Sciences USA 95:3140-3145.

Mulet, M., J. Lalucat, and E. Garcia-Valdes. 2010. DNA sequence-based analysis of the Pseudomonas species. Environ Microbiol 12:1513-1530.

Nishijyo, T., D. Haas, and Y. Itoh. 2001. The CbrA-CbrB two-component regulatory system controls the utilization of multiple carbon and nitrogen sources in Pseudomonas aeruginosa. Molecular Microbiology 40:917-931.

Norval, M., T. J. Simpson, and J. A. Ross. 2008. Urocanic acid and immunosuppression. Photochemistry and Photobiology 50:267-275.

Pérez-Losada, M., E. B. Brownea, A. Madsena, T. Wirth, R. P. Viscidi, and K. A. Crandall. 2006. Population genetics of microbial pathogens estimated from multilocus sequence typing (MLST) data. Infection, Genetics and Evolution 6:97-112.

Palleroni, N. J. 2010. The Pseudomonas story. Environmental Microbiology 12:1377-1383.

Rainey, P. B. 1999. Adaptation of Pseudomonas fluorescens to the plant rhizosphere. Environmental Microbiology 1:243-257.

Rainey, P. B., M. J. Bailey, and I. P. Thompson. 1994. Phenotypic and genotypic diversity of fluorescent pseudomonads isolated from field-grown sugar beet. Microbiology 140:873-884.

Revel, H. R. B., and B Magasanik. 1958. Utilization of the imidazole carbon 2 of histidine for the biosynthesis of purines in bacteria. Journal of Biological Chemistry 233:439-443.

Rico, A., and G. M. Preston. 2008. Pseudomonas syringae pv. tomato DC3000 uses constitutive and apoplast-induced nutrient assimilation pathways to catabolize nutrients that are abundant in the tomato apoplast. Molecular Plant-Microbe Interactions 21:269-282.

Ro¨ther, D., L. s. Poppe, S. Viergutz, B. Langer, and J. n. Re´tey. 2001. Characterization of the active site of histidine ammonia-lyase from Pseudomonas putida. European Journal of Biochemistry 268:6011-6019.

Sambrook, J., E. F. Fritsch, and T. Maniatis. 1989. Molecular Cloning: A Laboratory Manual. Cold Spring Harbor Laboratory Press, Cold Spring Harbor, NY.

Silby, M. W., A. M. Cerdeño-Tárraga, G. S. Vernikos, S. R. Giddens, R. W. Jackson, G. M. Preston, X.-X. Zhang, C. D. Moon, S. M. Gehrig, S. A. Godfrey, C. G. Knight, J. G. Malone, Z. Robinson, A. J. Spiers, S. Harris, G. L. Challis, A. M. Yaxley, D. Harris, K. Seeger, L. Murphy, S. Rutter, R. Squares, M. A. Quail, E. Saunders, K. Mavromatis, T. S. Brettin, S. D. Bentley, J. Hothersall, E. Stephens, C. M. Thomas, J. Parkhill, S. B. Levy, P. B. Rainey, and N. R. Thomson. 2009. Genomic and genetic analyses of diversity and plant interactions of Pseudomonas fluorescens. Genome Biology 10:R51.51-16.

Stanier, R. Y., N. J. Palleroni, and M. Doudoroff. 1966. The aerobic pseudomonads: a taxonomic study. Journal of General Microbiology 43:159-271.

Stover, C. K., X. Q. Pham, A. L. Erwin, S. D. Mizoguchi, P. Warrener, M. J. Hickey, F. S. L. Brinkman, W. O. Hufnagle, D. J. Kowalik, M. Lagrou, R. L. Garber, L. Goltry, E. Tolentino, S. Westbrock-Wadman, Y. Yuan, L. L. Brody, S. N. Coulter, K. R. Folger, A. Kas, K. Larbig, R. Lim, K. Smith, D. Spencer, G. K.-S. Wong, Z. Wu, I. T. Paulsenk, J. Reizer, M. H. Saier, R. E. W. Hancock, S. Lory, and M. V. Olson. 2000. Complete genome sequence of Pseudomonas aeruginosa PAO1, an opportunistic pathogen. Nature 406:959-964.

Tavanti, A., A. D. Davidson, M. J. Fordyce, N. A. R. Gow, M. C. J. Maiden, and F. C. Odds. 2005. Population structure and properties of Candida albicans, as determined by Multilocus Sequence Typing. Journal of Clinical Microbiology 43:5601-5613.

Thompson, I. P., A. K. Lilley, R. J. Ellis, P. A. Bramwell, and M. J. Bailey. 1995. Survival, colonization and dispersal of a genetically modified

Pseudomonas fluorescens (SBW25) in the phytosphere of field grown sugar beet. Biotechnology 13:1493–1497.

Waine, D. J., D. Honeybourne, E. G. Smith, J. L. Whitehouse, and C. G. Dowson. 2009. Cross-sectional and longitudinal multilocus sequence typing studies of Pseudomonas aeruginosa in cystic fibrosis sputum. Journal of Clinical Microbiology 47:3444-3448.

Williams, G. C. 1957. Pleiotropy, natural selection, and the evolution of senescence. Evolution 11:398-411.

Wilson, D. S., and J. Yoshimura. 1994. On the coexistence of specialists and generalists. The American Naturalist 144:692-707.

Zhang, X.-X., H. Chang, S. L. Tran, J. C. Gauntlett, G. M. Cook, and P. B. Rainey. 2011. Variation in transport explains polymorphism of histidine and urocanate utilization in a natural Pseudomonas population. Environmental Microbiology DOI: 10.1111/j.1462-2920.2011.02692.x.

Zhang, X.-X., A. George, M. J. Bailey, and P. B. Rainey. 2006. The histidine utilization (hut) genes of Pseudomonas fluorescens SBW25 are active on plant surfaces, but are not required for competitive colonization of sugar beet seedlings. Microbiology 152:1867-1875.

Zhang, X.-X., and P. B. Rainey. 2007. Genetic analysis of the histidine utilization (hut) genes in Pseudomonas fluorescens SBW25. Genetics 176:2165-2176.

Zhang, X.-X., and P. B. Rainey. 2008. Dual involvement of CbrAB and NtrBC in the regulation of histidine utilization in Pseudomonas fluorescens SBW25. Genetics 178:185-195.